Received: 22 November 2016 | Revised: 23 December 2016 | Accepted: 30 December 2016

DOI 10.1002/jmor.20653

RESEARCH ARTICLE

WILEY

Development of the skull and pectoral girdle in Siberian sturgeon, *Acipenser baerii*, and Russian sturgeon, *Acipenser gueldenstaedtii* (Acipenseriformes: Acipenseridae)

Peter Warth[1] | **Eric J. Hilton**[2] | **Benjamin Naumann**[1] | **Lennart Olsson**[1] | **Peter Konstantinidis**[3]

[1]Institut für Spezielle Zoologie und Evolutionsbiologie mit Phyletischem Museum, Friedrich-Schiller-Universität Jena, Germany

[2]Department of Fisheries Science, Virginia Institute of Marine Science, College of William & Mary, Gloucester Point, Virginia

[3]Department of Fisheries and Wildlife, Oregon State University, Corvallis, Oregon

Correspondence
Peter Warth, Institut für Spezielle Zoologie und Evolutionsbiologie mit Phyletischem Museum, Friedrich-Schiller-Universität Jena, Erbertstr. 1, 07743 Jena, Germany.
Email: Peter.Warth@uni-jena.de

Abstract

The head is considered the major novelty of the vertebrates and directly linked to their evolutionary success. Its form and development as well as its function, for example in feeding, is of major interest for evolutionary biologists. In this study, we describe the skeletal development of the cranium and pectoral girdle in Siberian (*Acipenser baerii*) and Russian sturgeon (*A. gueldenstaedtii*), two species that are commonly farmed in aquaculture and increasingly important in developmental studies. This study comprises the development of the neuro-, viscero- and dermatocranium and the dermal and chondral components of the pectoral girdle, from first condensation of chondrocytes in prehatchlings to the early juvenile stage and reveals a clear pattern in formation. The otic capsules, the parachordal cartilages, and the *trabeculae cranii* are the first centers of chondrification, at 8.4mm TL. These are followed by the mandibular, then the hyoid, and later the branchial arches. Teeth form early on the dentary, dermopalatine, and palatopterygoid, and then appear later in the buccal cavity as dorsal and ventral toothplates. With ongoing chondrification in the neurocranium a capsule around the brain and a strong rostrum are formed. Dermal ossifications start to form before closure of the dorsal neurocranial fenestrae. Perichondral ossification of cartilage bones occurs much later in ontogeny. Our results contribute data bearing on the homology of elements such as the lateral rostral canal bone that we regard homologous to the antorbital of other actinopterygians based on its sequence of formation, position and form. We further raise doubts on the homology of the posterior ceratobranchial among Actinopteri based on the formation of the hyoid arch elements. We also investigate the basibranchials and the closely associated unidentified gill-arch elements and show that they are not homologous.

KEYWORDS

Actinopterygii, basibranchial, bone, cartilage, homology

1 | INTRODUCTION

The vertebrate skull has long been of great interest to evolutionary biologists (de Beer, 1937; Goethe, 1820; Huxley, 1857; Oken, 1807; van Wijhe, 1882) and consists of endoskeletal (neurocranium and viscerocranium) and exoskeletal (dermatocranium) components. According to the new head hypothesis (Gans & Northcutt, 1983; Northcutt & Gans, 1983), the portions of the skull anterior to the notochord are formed by the neural crest and the posterior portions by mesoderm. Elements of the dermatocranium ossify without cartilaginous precursors, whereas elements of the endoskeleton often preform in cartilage and later ossify peri- and/or enchondrally. Embryologically, the dermatocranium is of mixed (mesodermal and neural crest) origin and can thereby be subdivided in two components. The exact position of the boundary between these components is inconsistent between vertebrate lineages (reviewed by Gross & Hanken, 2008; Piekarski, Gross, & Hanken, 2014; Santagati & Rijli, 2003). These differences and their implications for the homology of the bones across vertebrate taxa are not yet fully understood but can be used for homology statements (Maddin, Piekarski, Sefton, & Hanken, 2016). The viscerocranium derives from the neural crest

(e.g., Jiang, Iseki, Maxson, Sucov, & Morriss-Kay, 2002) and comprises the gill arches and their evolutionary derivatives (i.e., the hyoid and mandibular arch respectively). The neurocranium encapsulates the brain and is of mixed developmental origin. The formation of the anterior part of the neurocranium starts with the *trabeculae cranii* anteriorly, which are of neural crest origin, and posteriorly from the parachordals and the otic capsules, which are derived from cranial mesoderm (Couly, Coltey, & Le Douarin, 1992). The posteriormost part of the neurocranium, the occiput, is a derivation of the trunk and is formed from somitic mesoderm (Couly, Coltey, & Le Douarin, 1993). Recent research has demonstrated examples of putatively homologous structures in which the histogenesis and embryogenesis of structures differ between taxa (reviewed by Hirasawa & Kuratani, 2015). Understanding the development in different taxa is essential for a better understanding of the evolutionary changes that have occurred throughout vertebrates.

Due to their phylogenetic position as non-neopterygian actinopterygians, sturgeons, Acipenseridae, play an important role for our understanding of the evolution of vertebrate morphology in general. The Acipenseridae, together with paddlefishes (Polyodontidae) are grouped in the basal actinopterygian order Acipenseriformes. The order comprises about 27 extant species distributed throughout the Northern Hemisphere (Bemis, Findeis, & Grande, 1997; Birstein & Bemis, 1997). Sturgeon anatomy has interested morphologists since the 19th century and several reports on skeletal anatomy and development of different species are known (e.g., de Beer, 1925; Dillman & Hilton, 2015; Findeis, 1997; Hilton, 2005; Hilton, Dillman, Zhang, Zhang, & Zhuang, 2016; Hilton, Grande, & Bemis, 2011; Jollie, 1980; Nelson, 1969; Parker, 1881; Pehrson, 1944; Sewertzoff, 1928; see Hilton et al., 2011 for more references). The skeleton of sturgeons exhibits several peculiarities that are distinct from other extant vertebrates. Most apparent are the five rows of large dermal scutes along the body, the largely cartilaginous endoskeleton, the absence of vertebral centra, and the presence of numerous anamestic rostral bones covering an enlarged, pointed rostrum.

Although Acipenseriformes is widely viewed as the extant sister group to the Neopterygii (= Holostei + Teleostei; Grande, 2010), the phylogenetic relationships among species of Acipenseridae is still in flux (Bemis et al., 1997; Birstein, Doukakis, & DeSalle, 2002; Hilton et al., 2011; Krieger, Hett, Fuerst, Artyukhin, & Ludwig, 2008). Four morphologically distinct genera are currently recognized within the Acipenseridae: *Acipenser* (17 species), *Huso* (two species), *Pseudoscaphirhynchus* (three species), and *Scaphirhynchus* (three species). Mayden and Kuhajda (1996) grouped *Acipenser* and *Huso* in the subfamily Acipenserinae and *Pseudoscaphirhynchus* and *Scaphirhynchus* in the subfamily Scaphirhynchinae. In contrast Findeis (1997) ranked *Pseudoscaphirhynchus* + *Scaphirhynchus* as a tribe of the Acipenserinae and placed *Huso* in its own subfamily, Husinae. Based on molecular evidence, *Huso* was recovered (as both monophyletic and paraphyletic, depending on the study) in the genus *Acipenser* by several authors (e.g., Birstein & DeSalle, 1998; Birstein et al., 2002), although the species of *Huso* have only been formally classified within *Acipenser* by Vasil'eva, Vasil'ev, Shedko, and Novomodny (2009). Birstein et al. (2002), Dillman et al. (2007), and Hilton et al. (2011) recovered *Pseudoscaphirhynchus* as the sister group to *A. stellatus* and not as sister to *Scaphirhynchus*. The conflict in hypotheses of interrelationships among species of Acipenseridae highlights the importance of additional morphological and molecular data to address the interrelationships among these highly imperiled fishes. Among morphological data, ontogeny has proven to be a valuable source of characters (Bardin, Rouget, & Cecca, 2016) and the study and comparison of sturgeon development may add to our understanding of their phylogeny.

In this study, we describe the development of the Siberian and Russian sturgeons (*Acipenser baerii* Brandt 1869 and *Acipenser gueldenstaedtii* Brandt and Ratzeburg 1833, respectively), two Eurasian members of the Acipenseridae. *Acipenser baerii* is potamodromous (Bemis & Kynard, 1997; Birstein & Ruban, 2004) and was historically distributed over a large geographic area, ranging from the river drainages to the East Siberian Sea, westwards to the Ob river and the Kara Sea and inland to the Lake Baikal and rivers in Mongolia, Kazakhstan, and China (Birstein & Ruban, 2004; Ruban, 1997; Ruban & Zhu, 2010). Several subspecies are recognized in different rivers, with many of them threatened by anthropogenic impact (Ruban, 1997). *Acipenser gueldenstaedtii* is anadromous, with genetically distinct forms inhabiting the Caspian Sea and its tributary waters (Birstein & Ruban, 2004). Both species have been introduced into waters outside of their historical range and are known to hybridize with each other, as well as with other sturgeon species (e.g., Ludwig, Lippold, Debus, & Reinartz, 2009); hybridization is also known to occur among other sturgeon species (de la Herrán et al., 2001; Holčik, 1989; Tranah, Campton, & May, 2004). *Acipenser baerii* and *A. gueldenstaedtii* are reared and raised in hatcheries in Europe for caviar and food production (Bronzi, Rosenthal, Arlati, & Williot, 1999; Williot et al., 2001). This has augmented interest in several aspects of their natural history, not only related to hatchery and rearing questions (Gisbert & Ruban, 2003; Psenicka et al., 2008; Zelazowska, 2010) but also regarding their development (Gisbert, 1999; Rodríguez & Gisbert, 2001; Song & Song, 2012), including staging tables and descriptions of embryonic and larval stages (Leprévost, Azaïs, Trichet & Sire, 2016; Ginsburg & Dettlaff, 1991; Park, Lee Sang, Kim, & Kwon, 2013; Schmalhausen, 1991). As a contribution to the study of the vertebrate skull and to provide information that will help to solve the evolutionary relationships among the species, we document the skeletal development of the skull and the pectoral girdle of *A. baerii* and *A. gueldenstaedtii*, and provide an overview of the developmental timing of the differentiation of skeletal elements.

2 | MATERIAL AND METHODS

Developmental series of *A. baerii* and *A. gueldenstaedtii* were obtained from a commercial hatchery (Fischzucht Rhönforelle, Gersfeld, Hessen) between November 2013 and February 2014. Eggs and sperm had been taken from several individuals that had undergone hormonal treatment to stimulate gonadal ripening. After artificial insemination, eggs were raised at ambient temperature. Specimens were euthanized by an overdose of tricaine methanesulfonate (MS222) according to the animal welfare protocols at Friedrich-Schiller-Universität, Jena, and fixed in 4% paraformaldehyde for at least 24 hrs at 4°C.

Whole-mount clearing and staining for bone and cartilage with Alizarin red and Alcian blue respectively, was conducted following the protocol of Taylor and van Dyke (1985). Histological sections were prepared by embedding in paraffin and sectioning at 6 μm with a rotary microtome (Thermo Scientific Microm HM360) before staining following the Azan-Heidenhain technique (Romeis, 1989).

Timing of development, date of hatching, and growth rate of larvae can vary among offspring produced by different females and even within offspring of one pair of adults (Nathanailides, Tsoumani, Papazogloy, & Paschos, 2002). The resulting differences in timing of development are further enhanced by disparities in food uptake and water temperature. For ease of discussion and to make reliable comparisons within and between species, we staged specimens according to the total length (mm TL), but also report days post fertilization (dpf) in Materials Examined. Ossification of chondral bones often occurs late during development in sturgeons and many elements are therefore not described here. Skeletal terminology follows Hilton et al. (2011). Images were taken with an ICc Zeiss Camera attached to a Zeiss Discovery V20 stereomicroscope operated with Axiovision software. Backgrounds were cleaned and contrast was enhanced using Adobe Photoshop CS6. For Figure 10, 3D-reconstructions were prepared from μCT image stacks with Amira 5.4 (Visage Imaging, Berlin, Germany) and further processed with MAYA (Autodesk, San Rafael, California).

2.1 | Material examined

Institutional abbreviations follow Sabaj (2016).

2.1.1 | Cleared and stained whole mount specimens

Acipenser baerii Brandt 1869. VIMS 33602, developmental series of $n = 22$ cleared and stained specimens, representing 8.4–104.4 mm TL and 1–98 dpf; VIMS 33619, $n = 2$ c&s; VIMS 12083, $n = 1$ dried skeleton.

Acipenser gueldenstaedtii Brandt & Ratzeburg 1833. VIMS 33601, developmental series of $n = 15$ cleared and stained specimens, representing 8.2–101.0 mm TL and 1–98 dpf; VIMS 33620 ($n = 5$ c&s, 12.5–19.5 mm); VIMS 33621 ($n = 4$ c&s, 27.1–40.2 mm).

Other Acipenseridae. Materials listed in Hilton et al. (2011), as well as cleared and stained ontogenetic series of *Huso huso* and *A. ruthenus* (both uncatalogued at Institut für Spezielle Zoologie und Evolutionsbiologie mit Phyletischem Museum, Jena) were used for comparative purposes.

2.1.2 | Histological sections and μCT

Acipenser baerii: 13.2 mm TL, sectioned at 6 μm thickness in parasagittal plane and stained following the Azan-Heidenhain method. Slides are uncatalogued and deposited at the Institut für Spezielle Zoologie und Evolutionsbiologie mit Phyletischem Museum, Jena. 18.5 mm TL scanned with a phoenix nanotom (general electric, Boston, Massachusetts).

Lepisosteus osseus: 22.0 mm SL, material and image data is from Konstantinidis et al. (2015).

3 | RESULTS

We describe the skeletal development of the head and pectoral girdle of *A. baerii* and *A. gueldenstaedtii* separately. The order of these descriptions is as follows: the elements of the neurocranium followed by the visceral arches, then the dermatocranium and finally, the pectoral girdle. Figures 1–3 and Figures 5–7 show representative stages in the development of *A. baerii* and *A. gueldenstaedtii*, respectively. Figures 4 and 8 highlight details of dissected specimens.

3.1 | *Acipenser baerii*

3.1.1 | 8.4 mm TL to 11.0 mm TL (Figure 4a,b)

The first chondrocytes of the neurocranium appear dorsolateral and anterior to the notochord, where the base of the neurocranium will develop. These include the anteroventral part of the otic capsule and the anlage of the *trabecula cranii* (Figure 4a). Shortly after the anlage of the *trabecula cranii*, the parachordals appear and later fuse with the former (Figure 4b).

At the same time the first viscerocranial elements, the palatoquadrate and Meckel's cartilage, initially form in a mediolateral direction (Figure 4b). The palatoquadrate is s-shaped, curving first upward and then medially from the point where the jaw articulation will form. Meckel's cartilage is bent slightly toward the midline but a large gap exists between the left and right element.

3.1.2 | 12.5 mm TL

At this stage, the *trabeculae* and parachordals are joined to form the parachordal plate anterior to the notochord. The otic capsule is preformed in cartilage and vaguely outlined.

The palatoquadrate and Meckel's cartilage are well developed and broad laterally toward the jaw articulation. The dentary teeth are preformed, but not yet calcified.

3.1.3 | 12.8 mm TL (Figures 1a, 2a, and 3a)

In addition to the previous elements, the hyoid arch, the first branchial arch elements, and the scapulocoracoid cartilage begin to form.

A thin orbital cartilage, and an aggregation of chondrocytes in the rostral area, where the nasal capsule will be formed at a later stage are developed as independent entities (Figure 1a). The ventral part of the otic capsule is thicker and further advanced than the dorsal part and forms the facet for the single head of the hyomandibula.

The precursors of the dentition are now present in the upper jaw as well. All teeth are still not calcified. The long and slender shaft of the hyomandibula runs ventrally and attaches to the anlage of the interhyal (not visible in the figure, as connection was lost on left side of specimen during preparation), which connects to the jaw articulation anteriorly and the ventral part of the hyoid arch. A single basibranchial copula is located in the ventral midline, and a small hypohyal reaches from its anterolateral edge to connect with the anterior ceratohyal. The anterior ceratohyal is an elongated cartilage that becomes wider toward its rounded, slightly bifurcated distal end. The anterior process is the insertion point of the ceratomandibular ligament and a small

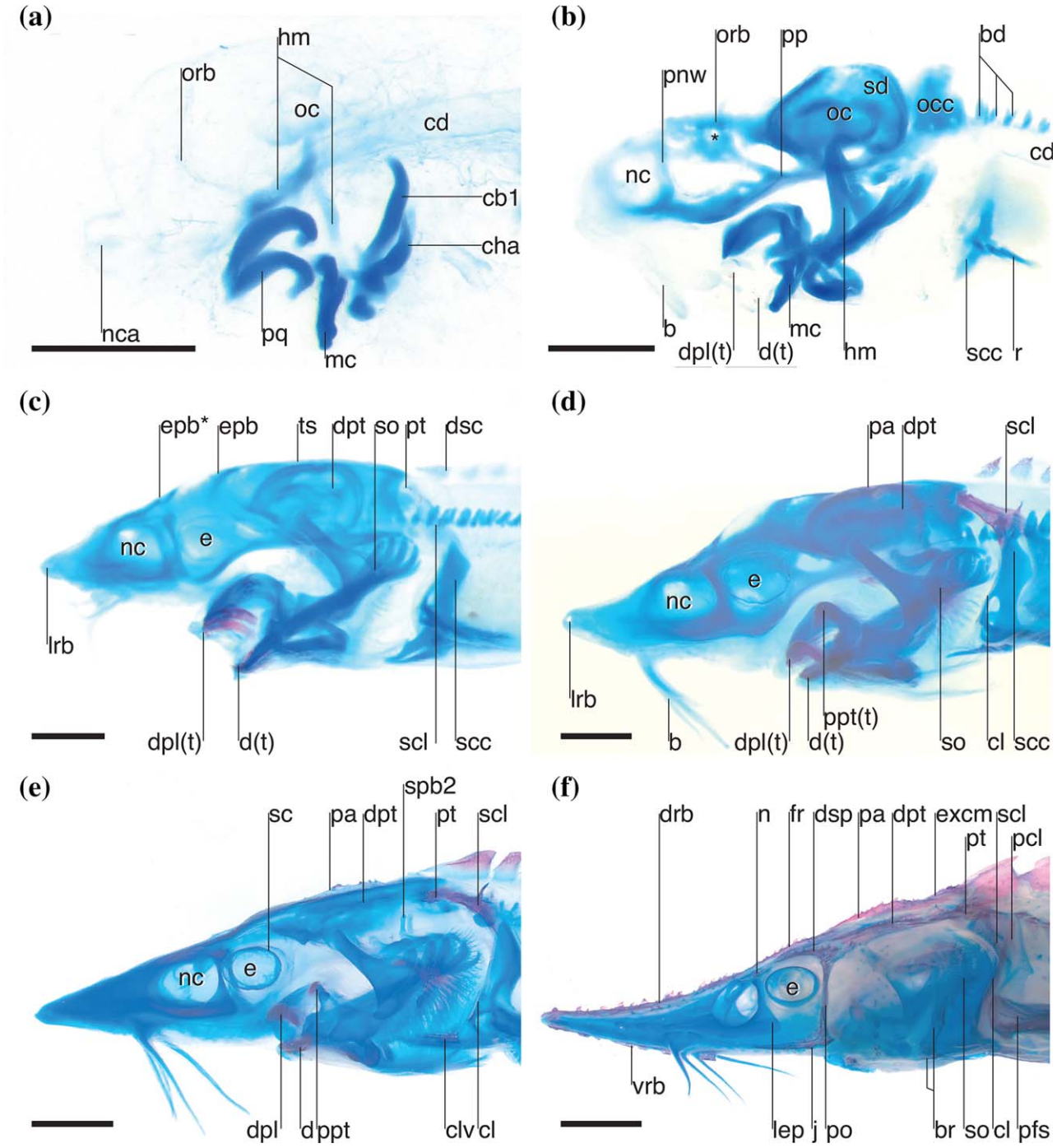

FIGURE 1 *Acipenser baerii*, cleared and stained series (VIMS 33602), showing head in lateral view, anterior facing left. (a) 12.8 mm TL (hm detached from interhyal on left side of specimen), scale is 1 mm. (b) 17.5 mm TL, scale is 1 mm. (c) 20.7 mm TL, scale is 1 mm. (d) 22.9 mm TL, scale is 1 mm. (e) 35.5 mm TL, scale is 2 mm. (f) 104 mm TL, scale is 5 mm. Abbreviations: b, barbel; bd, basidorsal; br, branchiostegal; cb, ceratobranchial; cd, notochord; cha, anterior ceratohyal; cl, cleithrum; clv, clavicle; d, dentary; d(t), toothed dentary; dpl, dermopalatine; dpl(t), toothed dermopalatine; dpt, dermopterotic; drb, dorsal rostral bones; dsc, dorsal scute; dsp, dermosphenotic; e, eye; epb, epiphyseal bridge; epb*, epiphyseal bridge of Holmgren & Stensiö, 1936; excm, median extrascapular; fr, frontal; hm, hyomandibula; j, jugal; lep, lateral ethmoid process of the neurocranium; lrb, lateral rostral canal bone; mc, Meckel's cartilage; n, nasal; nc, nasal capsule; nca, anlage of nasal capsule; oc, otic capsule; occ, occiput; orb, orbital cartilage; pa, parietal; pcl, postcleithrum; pfs, "pectoral fin spine"; pnw, posterior nasal wall; po, postorbital; pp, parachordal plate; ppt, palatopterygoid; ppt(t), toothed palatopterygoid; pq, palatoquadrate; pt, posttemporal; r, proximal radial; sc, scleral cartilage; scc, scapulocoracoid cartilage; scl, supracleithrum; sd, semicircular duct; so, subopercle; spb2, suprapharyngobranchial 2; ts, *tectum synoticum*; vrb, ventral rostral bones; * *canalis opticus*

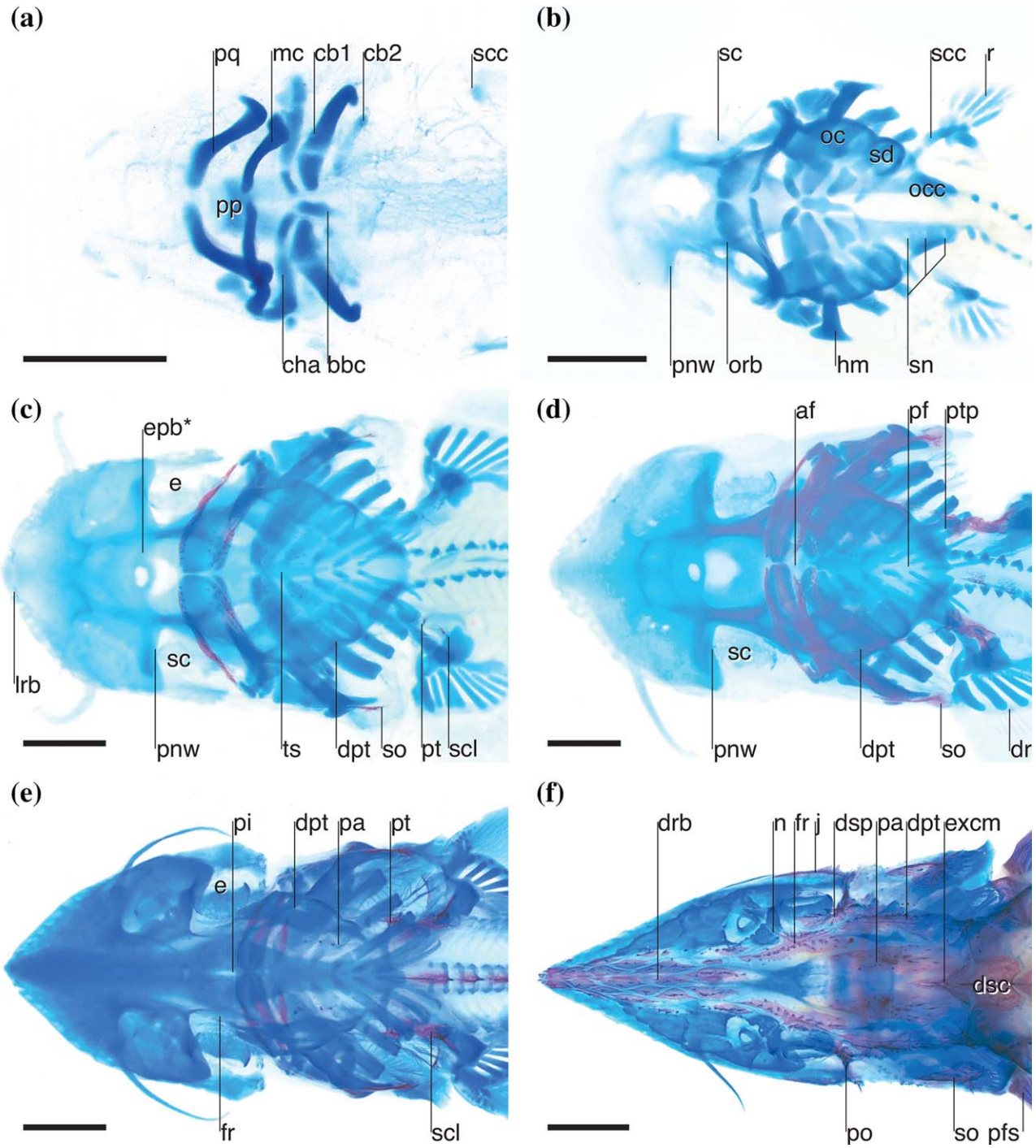

FIGURE 2 *Acipenser baerii*, cleared and stained series (VIMS 33602), showing head in dorsal view, anterior facing left. (a) 12.8 mm TL, scale is 1 mm. (b) 17.5 mm TL, scale is 1 mm. (c) 20.7 mm TL, scale is 1 mm. (d) 22.9 mm TL, scale is 1 mm. (e) 35.5 mm TL, scale is 2 mm. (f) 104 mm TL, scale is 5 mm. Abbreviations: af, anterior fontanelle; bbc, basibranchial copula; cb, ceratobranchial; cha, anterior ceratohyal; dpt, dermopterotic; dr, distal radial; drb, dorsal rostral bones; dsc, dorsal scute; dsp, dermosphenotic; e, eye; epb*, epiphyseal bridge of Holmgren & Stensiö, 1936; excm, median extrascapular; fr, frontal; hm, hyomandibula; j, jugal; lrb, lateral rostral canal bone; mc, Meckel's cartilage; n, nasal; oc, otic capsule; occ, occiput; orb, orbital cartilage; pa, parietal; pf, posterior fontanelle; pfs, "pectoral fin spine"; pi, pineal fontanelle; pnw, posterior nasal wall; po, postorbital; pp, parachordal plate; pq, palatoquadrate; pt, posttemporal; ptp, posttemporal process; r, proximal radial; sc, scleral cartilage; scl, supracleithrum; scc, scapulocoracoid cartilage; sd, semicircular duct; sn, spinal occipital nerve exit; so, subopercle; ts, *tectum synoticum*

condensation of chondrocytes distal to the posterior process represents the posterior ceratohyal. At this stage it is positioned loosely between the anterior ceratohyal and the interhyal. The elements of the first branchial arch are more massive than the elements of the hyoid arch (Figure 3a). Posterior to the hypohyal, hypobranchial 1 attaches to the basibranchial copula and becomes slightly wider laterally. There is

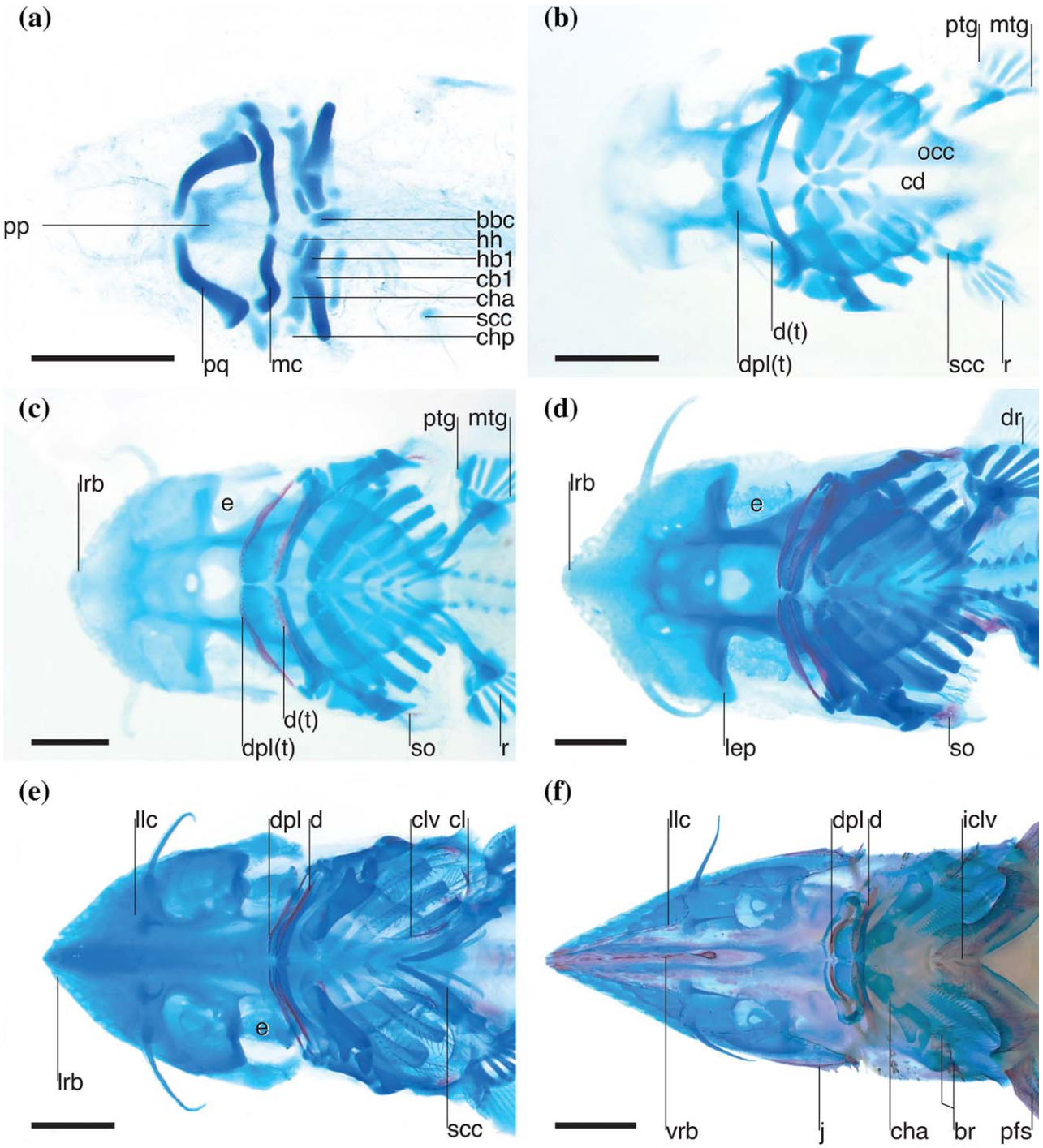

FIGURE 3 *Acipenser baerii*, cleared and stained series (VIMS 33602), showing head in ventral view, anterior facing left. (a) 12.8 mm TL, scale is 1 mm. (b) 17.5 mm TL, scale is 1 mm. (c) 20.7 mm TL, scale is 1 mm. (d) 22.9 mm TL, scale is 1 mm. (e) 35.5 mm TL, scale is 2 mm. (f) 104 mm TL, scale is 5 mm. Abbreviations: bbc, basibranchial copula; br, branchiostegal; cb, ceratobranchial; cd, notochord; cha, anterior ceratohyal; chp, posterior ceratohyal; cl, cleithrum; clv, clavicle; d, dentary; d(t), toothed dentary; dpl, dermopalatine; dpl(t), toothed dermopalatine; dr, distal radials; e, eye; hb, hypobranchial; hh, hypohyal; iclv, interclavicle; j, jugal; lep, lateral ethmoid process of the neurocranium; llc, lateral line canal; lrb, lateral rostral canal bone; mc, Meckel's cartilage; mtg, metapterygium; occ, occiput; pfs, "pectoral fin spine"; pp, parachordal plate; pq, palatoquadrate; ptg, propterygium; r, proximal radial; scc, scapulocoracoid cartilage; so, subopercle; vrb, ventral rostral bones

no clear gap between hypobranchial 1 and ceratobranchial 1, although a line of lighter staining in the specimen marks the boundary between the elements. The distal part of ceratobranchial 1 curves upward. Hypobranchial 2 and ceratobranchial 2 are markedly less developed than the respective elements of the first branchial arch and attach to the posterolateral part of the basibranchial copula.

The scapulocoracoid cartilage is a small rounded condensation of chondrocytes (Figure 2a).

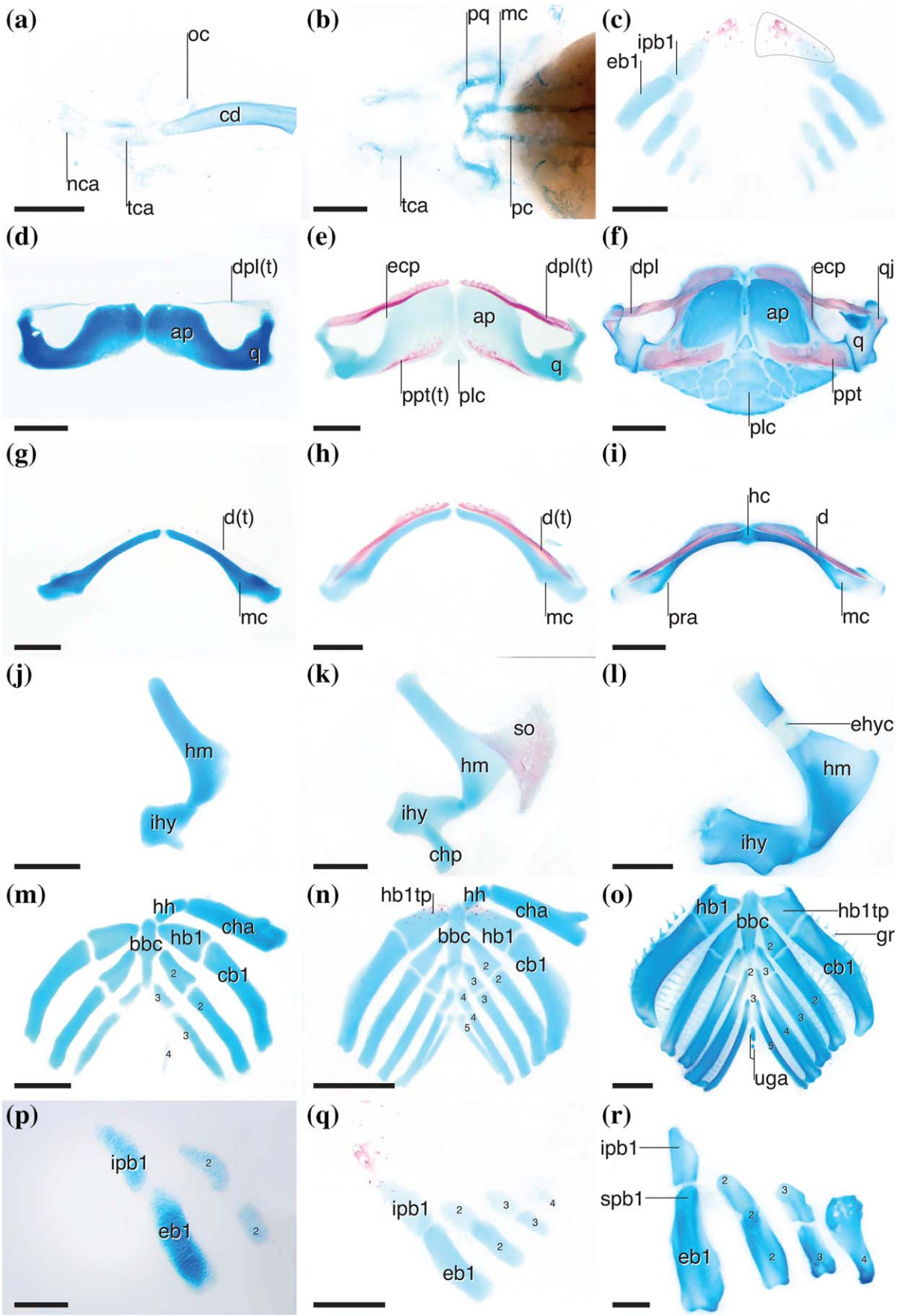
(a)
oc
cd
nca
tca
(b)
pq
mc
tca
pc
(c)
ipb1
eb1
(d)
dpl(t)
ap
q
(e)
ecp
dpl(t)
ap
q
ppt(t)
plc
(f)
dpl
ecp
qj
ap
q
ppt
plc
(g)
d(t)
mc
(h)
d(t)
mc
(i)
hc
d
pra
mc
(j)
hm
ihy
(k)
so
hm
ihy
chp
(l)
ehyc
hm
ihy
(m)
hh
cha
bbc
hb1
cb1
(n)
hb1tp
hh
cha
bbc
hb1
cb1
(o)
hb1
hb1tp
bbc
gr
cb1
uga
(p)
ipb1
eb1
(q)
ipb1
eb1
(r)
ipb1
spb1
eb1

FIGURE 4.

3.1.4 | 17.5 mm TL (Figures 1b, 2b, 3b, and 4d,g,j,m,p)

The neurocranium forms a cartilaginous case for the brain and sensory organs ventrally and laterally but remains open dorsally. The rostroethmoidal region is clearly delineated by cartilage, although the anterior part is diffuse and just starting to condense. It appears convex in dorsal view (Figure 2b) and bulbous in lateral view (Figure 1b). The posterior nasal wall (*lamina orbitonasalis*) is formed and demarcates the border between the nasal and orbital regions. From the posterior nasal wall, the orbital cartilage forms a posterodorsal bridge which, before joining the otic capsule, extends ventrally to form a ring around the optic nerve, and continues posteroventrally to join the parachordal plate. At this stage the scleral cartilage is visible for the first time, although just as a diffuse layer of chondrocytes that surrounds the eye (Figure 1b). The parachordals extend posteriorly to connect with the otic capsule and the developing occipital region of the neurocranium. The otic capsule is well developed but the large semicircular ducts are not yet fully enclosed in cartilage dorsomedially. The occipital region develops by fusion of basidorsals. From both sides of the notochord, they reach dorsomedially but do not meet in the midline. They border the neural tube laterally and connect with the otic capsule via a cartilaginous bridge anterodorsally. Three foramina for the spinal occipital nerves 1–3 pierce each side of the occiput (Figure 2a).

The first bony elements are ossifications of the mandibular arch: the dentary in the lower jaw, covering the anterior surface of Meckel's cartilage (Figure 4g) and the dermopalatine and palatopterygoid on the anterolateral and posterior margins of the palatoquadrate, respectively (Figures 1b and 4d). Teeth are present on all three elements (Figure 4d, g). The dorsal shaft of the hyomandibula is long and slender as described in the previous stages but has a posterior outgrowth that extends ventrally (Figure 4j). The interhyal is broad and points anteriorly where it articulates with the mandibular arch. A groove on its medial surface receives the triangular posterior ceratohyal. The anterior ceratohyal is long and broad. At this stage, the ventral portion of the gill arches includes the elements of the third gill arch: the hypobranchial and ceratobranchial 3. Ceratobranchial 4 is weakly developed and present on the right side of the specimen only. Hypobranchial 2 is clearly separated from ceratobranchial 2 (Figure 4m). A tooth plate is supported by hypobranchial 1 (not illustrated). Elements of the dorsal gill arches appear in the first two gill arches (Figure 4p): the epibranchials, infrapharyngobranchials, and suprapharyngobranchials. The suprapharyngobranchials (not shown) are weakly developed and consist of a condensation formed by a few chondrocytes dorsal to the enlarged proximal parts of the epibranchials. The condensation on the right side is slightly more advanced than on the left side.

The pectoral girdle is substantially developed compared to the previous stage. The scapulocoracoid cartilage is extended to form a dorsoventral bar with an attached pectoral fin. The latter is supported by the cartilaginous propterygium, metapterygium, and the proximal radials (Figure 3b).

3.1.5 | 20.2 mm TL (Figures 1c, 2c, 3c, and 4c,e,h,k,n,q)

The rostroethmoidal region has become more massive, with the rostrum and the large nasal capsule being well differentiated (Figure 1c). The posterior nasal wall forms a straight anterior border of the orbital region and dorsomedially forms part of a bridge (= epiphyseal bridge of Holmgren & Stensiö, 1936), which continues medially. Posterior to this bridge, a gap persists in the dorsal midline of the neurocranium. The gap is laterally constricted and thereby subdivided into three parts (pineal foramen, and the anterior and posterior fontanelles) by the epiphyseal bridge and the *tectum synoticum* that have started to develop at the interface of the orbital and otic regions and at the mid-level of the otic region, respectively. The occiput is not fully closed dorsally but bears a posttemporal process laterally; an additional basidorsal is fused posteriorly. The scleral cartilage is more pronounced than in the previous stage (Figure 2c) and the otic capsule is dorsally enclosed in cartilage.

In the upper jaw, the small ectopterygoid is ossified as a slender rod on the lateral surface of the *pars autopalatina* (Figure 4e). The dermopalatine, palatopterygoid, dentary, and their associated teeth have become more strongly developed than in the previous stage (Figure 4h). The bases of the teeth are firmly attached to the underlying bone. The palatopterygoid stretches on the posterior margin of the palatoquadrate cartilage from the *pars quadrat*a to the *pars*

FIGURE 4 *Acipenser baerii*, detailed views of early stages and dissected specimens (VIMS 33602), highlighting elements of mandibular, hyoid and gill arches (anterior facing upwards unless indicated differently). (a) 8.4 mm TL, head in dorsolateral view, anterior facing left, scale is 0.5 mm. (b) 8.5 mm TL, head in dorsal view, anterior facing left, scale is 0.5 mm. (c) 20.2 mm TL, dorsal gill arches in ventral view, scale is 0.5 mm, drawn line indicates extension of toothplate. (d) 17.5 mm TL, upper jaw in ventral view, scale is 0.5 mm. (e) 20.2 mm TL, upper jaw in ventral view, scale is 0.5 mm. (f) 104 mm TL, upper jaw in ventral view, scale is 2 mm. (g) 17.5 mm TL, lower jaw in dorsal view, scale is 0.5 mm. (h) 20.2 mm TL, lower jaw in dorsal view, scale is 0.5 mm. (i) 104 mm TL, lower jaw in dorsal view, scale is 2 mm. (j) 17.5 mm TL, hyomandibula in lateral view, anterior facing left, scale is 0.5 mm. (k) 20.2 mm TL, hyomandibula in lateral view, anterior facing left, scale is 0.5 mm, (l) 104 mm TL, hyomandibula in lateral view, anterior facing left, scale is 2 mm. (m) 17.5 mm TL, ventral portion of gill arches in dorsal view, scale is 0.5 mm. (n) 20.2 mm TL, ventral portion of gill arches in dorsal view, scale is 1 mm. (o) 104 mm TL, ventral portion of gill arches in dorsal view, scale is 2 mm. (p) 17.5 mm TL, dorsal portion of gill arches in ventral view, anterior facing left, scale is 0.5 mm. (q) 20.2 mm TL, dorsal portion of gill arches in ventral view, anterior facing left, scale is 0.5 mm. (r) 104 mm TL, dorsal portion of gill arches in ventral view, anterior facing left, scale is 1 mm. Abbreviations: ap, *pars autopalatina* of palatoquadrate cartilage; bbc, basibranchial copula; cb, ceratobranchial; cd, notochord; cha, anterior ceratohyal; chp, posterior ceratohyal; d, dentary; d(t), toothed dentary; dpl, dermopalatine; dpl(t), toothed dermopalatine; eb, epibranchial; ecp, ectopterygoid; ehyc, external hyoid arch cartilage; gr, gillraker; hb, hypobranchial; hb1tp, toothplate on hypobranchial 1; hc, hyaline cartilage; hh, hypohyal; hm, hyomandibula; ihy, interhyal; ipb, infrapharyngobranchial; mc, Meckel's cartilage; nca, anlage of nasal capsule; oc, otic capsule; pc, parachordals; plc, palatal complex; ppt, palatopterygoid; ppt(t), toothed palatopterygoid; pra, prearticular; pq, palatoquadrate; q, *pars quadrata* of palatoquadrate cartilage; qj, quadratojugal; so, subopercular; spb, suprapharyngobranchial; tca, anlage of *trabecula cranii*; uga, unidentified gill-arch element

autopalatina. It extends anteromedially on the ventral surface of the *pars autopalatina* and additional teeth are formed on this extending edge. Posterior to the palatoquadrate, the palatal complex is now present as a single median cartilage plate. At this stage the hyomandibula is of the typical shape present in adult acipenserids, with a well-developed ventral hyomandibular cartilaginous blade (Figure 4k). Hypobranchial 3 encompasses the basibranchial copula ventrally with an anteroventral process, contacting its antimere in the midline. Anteromedial to ceratobranchial 4, a separate hypobranchial 4 is now present and ceratobranchial 5 is formed posteriorly. Dorsally, the epibranchial series is completed by the appearance of epibranchials 3 and 4. The size of the four epibranchials decreases in an anteroposterior direction (Figure 4q). Infrapharyngobranchial 3 is also present now, as are two small condensations of chondrocytes dorsal to the proximal parts of epibranchials 1 and 2, which represent suprapharyngobranchials 1 and 2, respectively (not shown). Small toothplates cover hypobranchial 1 (Figure 4n) and the region around infrapharyngobranchial 1 on the dorsal roof of the gill cavity (= the parasphenoid tooth plate; Figure 4c).

The first dermatocranial elements to appear are the dermopterotic, the lateral rostral canal bone, and the subopercle. The lateral rostral canal bone is a small canal bone at the anterior border of the rostrum. The dermopterotic is a thin, elongate element on the dorsolateral surface of the otic capsule. The thin triangular subopercle is large and flat (Figures 3c and 4k).

Posterior to the head, the first dorsal scutes appear in the dorsal-fin fold and a weakly ossified supracleithrum extends the scapulocoracoid cartilage dorsally and overlaps with the small posttemporal. The pro- and metapterygium and the proximal radials that project distally from these are well differentiated and more prominent than in the previous stages. The propterygium extends anteriorly to reach to the point where the pectoral-fin spine will eventually develop.

3.1.6 | 22.9 mm TL (Figures 1d, 2d, and 3d)

The rostrum is slightly elongated and more pointed anteriorly compared to the previous stage. Posteriorly, the chondrocranium is consolidated, and the dorsal roof starts to close as the *tectum synoticum* separates a large anterior fontanelle from a smaller posterior one in the occipital area. The occipital area is fully fused to the otic region and the dorsomedial crest as well as the posttemporal process consolidate. Posterior to the occiput, the basidorsals form around the spinal cord. The anteriormost is in touch with the occiput and gets incorporated subsequently. The teeth on the dentary and dermopalatine are less prominent than in earlier stages. The triangular ectopterygoid is enlarged and more massive. Suprapharyngobranchials 1 and 2 are well differentiated but do not articulate firmly with the neurocranium. The frontal above the eye is faint and weak. The parietal is a thin plate with a small crest, covering the dorsal part of the otic capsule (Figure 1d). The supracleithrum is broader and contacts the posttemporal, thereby linking the pectoral girdle to the head (Figures 1d and 2d). Ventral to the posttemporal, the cleithrum and the clavicle are present as thin ossifications. The first condensations of the distal radials are present at the tip of some of the proximal radials support the pectoral fin (Figure 3d).

3.1.7 | 35.4 mm TL (Figures 1e, 2e, and 3e)

The rostrum is now a massive and elongated cartilaginous block and the orbital region is partially roofed by cartilaginous crests extending laterally. Anteriorly a pointed *processus preorbitalis* extends from the nasal capsule and posteriorly a broad and pierced *processus postorbitalis cranii* reaches from the otic area into the orbital region. The anterior fontanelle is almost closed. The occiput is elongated posteriorly around the notochord in specimens slightly smaller than the one described here (30.5 mm TL), and an additional basidorsal is incorporated into the occipital region. The scleral cartilage forms a ring around the eye.

The left and right rami of Meckel's cartilage are now connected by a hyaline cartilage. The teeth of the dentary and dermopalatine are no longer present, but their former position can still be inferred from cavities in the underlying bones. The palatopterygoid lacks teeth posteriorly, but a few teeth are still present in the anterior part that covers the ventral surface of the *pars autopalatina*. Chondrification of the palatal complex is advanced, as lateral to the previously described median plate, a smaller plate has formed (see Figure 4e,f, for clarification of the palatal complex in a smaller and a larger specimen, respectively). Posterior to the large anterior basibranchial copula, two additional basibranchial copulae appeared. On the distal tip of ceratobranchial 4 a posteromedially directed process has formed. Epibranchial 4 is club shaped, attaching its slender distal part to ceratobranchial 4 and then extending the element proximally. Each of the epibranchials 1–3 bears a dorsally directed uncinate process that is extended by the suprapharyngobranchials in the first two gill arches. Suprapharyngobranchial 1 is a short but massive element and suprapharyngobranchial 2 is a long, slender, fingerlike cartilage connecting to the ventrolateral surface of the occipital region (Figure 1e). Gill rakers are only present on the anterior margin of ceratobranchial 1.

The frontal extends from the level of the nasal capsule to the parietal medially and the dermopterotic laterally. On the frontal, the bony canal around the sensory canal has begun to form and is prolonged anteriorly by a small tube between the anterior and posterior nares. The parietal is ornamented by small protuberances and extends from the posterior border of the orbital region to the occipital area (Figure 1e). The dermopterotic is expanded and forms a plate that bears the supratemporal canal, which continues posteriorly into the posttemporal. On the posteroventral corner of the orbital region, the jugal (ventral) and the postorbital (dorsal) form around the infraorbital sensory canal; these bones, however, are well separated from each other at this stage. The dermosphenotic is weakly developed above the orbit and lateral to the frontal.

Ventral to the supracleithrum the suprascapular cartilage is present (Figure 3e). The pectoral-fin spine has started to form anterodistal to the propterygium. In this area, several small cartilages have also formed (Figure 2e). Posteriorly, the distal radials are well differentiated.

3.1.8 | 104.0 mm TL (Figures 1f, 2f, 3f, and 4f,i,l,o,r)

The rostrum has elongated considerably and most of the chondrocranium is covered by heavily ornamented dermal dorsal rostral bones.

Their numerous sharp and thorn-like protuberances give the head a rough appearance. The pineal fontanelle, located in the chondrocranium between the frontals, is now closed. On the ventral side, a prominent median *trabecular processus* is formed.

Along the posterior edge of Meckel's cartilage, a small prearticular is present. The dentary and the dermopalatine are completely edentulous at this stage, although the palatopterygoid still bears weakly formed teeth on its anterior margin. A small quadratojugal is present dorsal to the jaw articulation, covering the lateral part of the *pars quadrata* of the palatoquadrate cartilage. The palatal complex is enlarged compared to the previous stage and consists of several irregularly shaped cartilaginous plates. A perichondral ossification has developed around the dorsal shaft of the hyomandibular cartilage and superficial to it there are several small external cartilages. The anterior ceratohyal starts to ossify in the midline. In the fourth gill arch, only one ventral element, ceratobranchial 4, is present (i.e., a separate hypobranchial is absent). Additional posterior median cartilages are present in the ventral portion of the gill arches. The tooth plate of hypobranchial 1 and the parasphenoid tooth plate in the dorsal gill cavity are still present but are weaker and smaller than in the previous stage. Gill rakers are present on both margins of the gill arches (ceratobranchial 5 only bears anterior gill rakers).

The dorsal part of the rostrum is covered by several dorsal rostral bones, which extend to the height of the nasal capsule posteriorly. They are restricted in their lateral extension, leaving a gap directly anterior to the nasal capsules. Anterolateral to the frontal, a nasal is now present and the parietals are separated posteriorly by a median extrascapular. The parasphenoid is present and well developed. It is deeply forked posteriorly and extends anteriorly from the pectoral girdle to the level of the jugal. On either side of the parasphenoid, an ascending process extends toward the dermosphenotic. An elongate median anterior process becomes embedded in the cartilage of the rostrum (*processus basalis medialis*). The anterior tip of this process contacts the posteriormost ventral rostral bone. Five median ventral rostral bones extend from the tip of the rostrum to the nasal capsule; the anteriormost ventral rostral bones are flanked by smaller posterior ones. Several ossifications around the rostral sensory canal delineate its path from the lateral rostral canal bones in an s-curve around the barbels to the jugal to become the infraorbital sensory canal. The jugal is much larger than in previous stages and contacts the postorbital, through which the infraorbital lateral line canal passes dorsally before it continues to the dermosphenotic and then on to the dermopterotic as the supratemporal sensory canal. Small ossifications in the skin are present in the area between the postorbital and the subopercle. Two thin plate-like branchiostegals are present ventral to the subopercle.

The pectoral girdle is strong and much advanced in respect to the previous stage. The pectoral-fin spine is well developed and articulates with the robust cleithrum. An interclavicle is present between the left and right clavicles. A postcleithrum is present posterior to the supracleithrum.

3.2 | *Acipenser gueldenstaedtii*

3.2.1 | 14 mm TL (Figures 5a, 6a, and 7a)

At this stage, the left and right parachordals have formed and are positioned lateral to the notochord. The parachordals are fused at their anterior tips to form a parachordal plate. Anteriorly, the *trabecula cranii* is incorporated into this cartilaginous complex and extends farther into the rostroethmoidal area (Figure 7a). The structure is laterally constricted (= prootic incisure of de Beer, 1925) at the level of the eye. Dorsal to this, the anlage of the orbital cartilage is present. Posteriorly, the otic capsule is formed, with a strong ventral base, from which a wall rises laterally and becomes progressively weaker dorsally, leaving the dorsal part of the neurocranium open.

The viscerocranium consists of the mandibular, hyoid, and first branchial arches. The palatoquadrate and Meckel's cartilages are present, but the left and right elements of each are separated in the midline (Figure 7a). The palatoquadrate is higher anteriorly than posteriorly and is perpendicular to the body axis. It then curves posterolaterally and widens toward the articulation with Meckel's cartilage. The anteromedial tip of Meckel's cartilage curves slightly anterodorsally. Tooth anlagen are present at the tips of the upper and lower jaws. The elements of the hyoid arch are well differentiated. The hyomandibula connects to the ventral part of the otic capsule via a distinct facet. The interhyal connects the anteroventral tip of the hyomandibula with the jaw articulation. At the ventral tip of the hyomandibula, a small posterior ceratohyal is formed and contacts the anterior ceratohyal. The hypohyal attaches the anterior ceratohyal to the anterolateral edge of the basibranchial copula in the midline. Farther posteriorly, hypobranchials 1 and 2 are present, of which hypobranchial 1 is twice as large as hypobranchial 2. Ceratobranchials 1 and 2 articulate distally with these and are slender rods that carry gill filaments (Figures 5a, 6a, and 7a).

The scapulocoracoid cartilage has started to form and is represented by a small condensation of chondrocytes.

3.2.2 | 16.8 mm TL (Figures 5b, 6b, 7b, and 8d,g,j,m,p)

The rostroethmoidal region is distinct at this stage, and forms an anterolateral extension of the *trabecula cranii* and the parachordal plate. The rounded anterior margin of the rostrum is weakly developed and appears diffuse in dorsal view (Figure 6b). Posteriorly, the cartilage becomes larger, forming prominent lateral ethmoid processes and posterior nasal walls. Its posterodorsal margin is in contact with the orbital cartilage, which extends posteriorly and projects ventrally to contact the parachordal plate and dorsally to join the otic capsule. The otic capsule is almost enclosed dorsally and the semicircular ducts are clearly visible (Figure 5b). Posteriorly, the occipital region is now formed by basidorsals on both sides of the notochord, reaching around the neural tube and rising dorsally to the height of the skull roof. The scleral cartilage forms a thin ring around the eye (Figure 6b).

The margins of the palatoquadrate are defined by two thin and weakly calcified, dentulous bones: the dermopalatine anteriorly and the palatopterygoid posteriorly (Figure 8d). Similarly, in the lower jaw the dentary covers the anterior part of Meckel's cartilage and carries small, pointed teeth in its midsection (Figure 8g). The hyomandibula is broader ventrally than in the previous stage (Figure 8j). The anterior

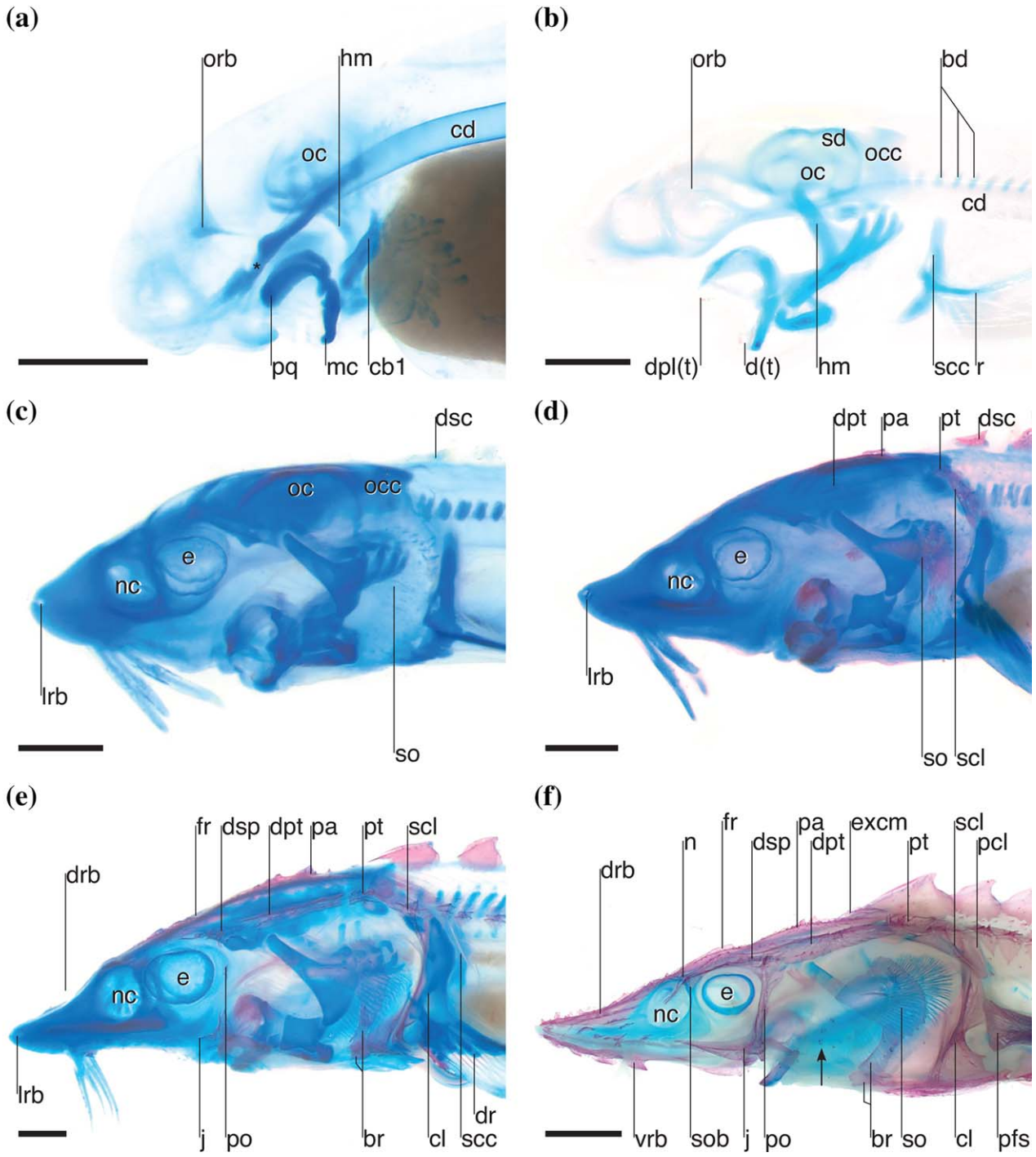

FIGURE 5 *Acipenser gueldenstaedtii*, cleared and stained series (VIMS 33601), showing head in lateral view, anterior facing left. (a) 14 mm TL, scale is 1 mm. (b) 16.8 mm TL, scale is 1 mm. (c) 19.8 mm TL, scale is 1 mm. (d) 20.5 mm TL, scale is 1 mm. (e) 31 mm TL, scale is 2 mm. (f) 101 mm TL, scale is 5 mm, arrow points out dermal ossicles. Abbreviations: bd, basidorsal; br, branchiostegal; cb, ceratobranchial; cd, notochord; cl, cleithrum; d(t), toothed dentary; dpl(t), toothed dermopalatine; dpt, dermopterotic; dr, distal radials; drb, dorsal rostral bones; dsc, dorsal scute; dsp, dermosphenotic; e, eye; excm, median extrascapular; fr, frontal; hm, hyomandibula; j, jugal; lrb, lateral rostral canal bone; mc, Meckel's cartilage; n, nasal; nc, nasal capsule; oc, otic capsule; occ, occiput; orb, orbital cartilage; pa, parietal; pcl, postcleithrum; pfs, "pectoral fin spine"; po, postorbital; pq, palatoquadrate; pt, posttemporal; r, proximal radial; scc, scapulocoracoid cartilage; scl, supracleithrum; sd, semicircular duct; so, subopercle; sob, supraorbital; vrb, ventral rostral bones; *, prootic incisure

ceratohyal is also broader than in earlier stages and possesses an anterior process that receives the ceratomandibular ligament. A tooth plate is present on hypobranchial 1 and the ventral portion of the branchial skeleton now contains hypobranchial 3 and 4 and ceratobranchial 3 and 4 in addition to the more anterior elements (Figure 8m). Dorsal to this, epibranchials 1 to 4 are present and decrease in size from anterior

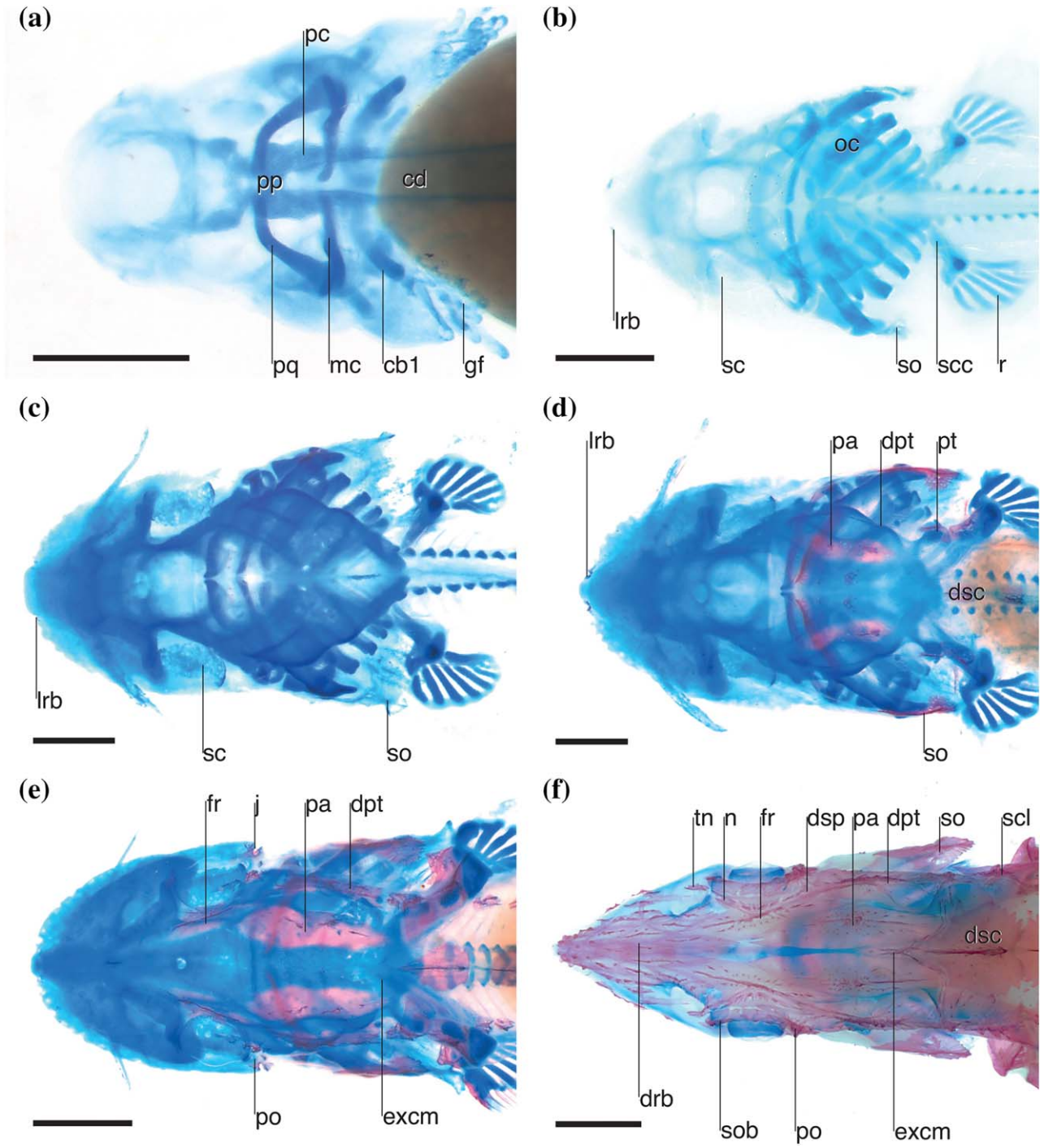

FIGURE 6 *Acipenser gueldenstaedtii*, cleared and stained series (VIMS 33601), showing head in dorsal view, anterior facing left. (a) 14 mm TL, scale is 1 mm. (b) 16.8 mm TL, scale is 1 mm. (c) 19.8 mm TL, scale is 1 mm. (d) 20.5 mm TL, scale is 1 mm. (e) 31 mm TL, scale is 2 mm. (f) 101 mm TL, scale is 5 mm. Abbreviations: cb, ceratobranchial; dpt, dermopterotic; drb, dorsal rostral bones; dsc, dorsal scute; dsp, dermosphenotic; excm, median extrascapular; fr, frontal; gf, gill filaments; j, jugal; lrb, lateral rostral canal bone; mc, Meckel's cartilage; n, nasal; oc, otic capsule; pa, parietal; pc, parachordal; po, postorbital; pp, parachordal plate; pq, palatoquadrate; pt, posttemporal; r, proximal radial; sc, scleral cartilage; scc, scapulocoracoid cartilage; scl, supracleithrum; so, subopercle; tn, tubular nasal

to posterior, with the posteriormost element being represented by a small, roundish condensation of chondrocytes. Infrapharyngobranchials 1–3 are present and decrease in size in an anteroposterior direction. The medial portions of the left and right infrapharyngobranchial 1 are covered by the parasphenoid tooth plates in the dorsal gill cavity (see drawn line in Figure 8p). The tooth plates extend medially, almost meeting their antimere.

The scapulocoracoid cartilage has elongated significantly and the pectoral fin attaches to it. The fin is supported by the propterygium and metapterygium, and by a series of proximal radials (Figure 7b).

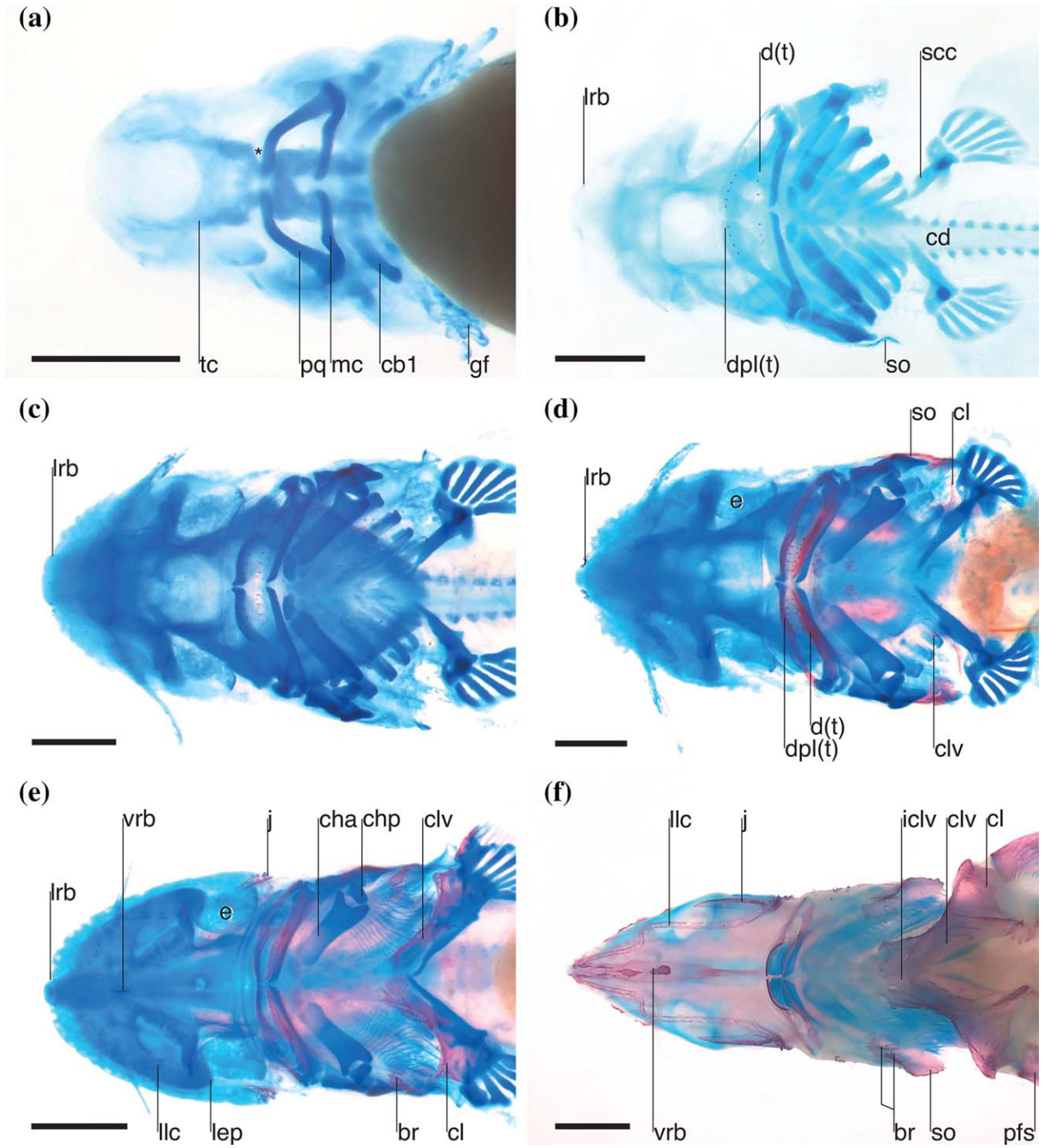

FIGURE 7 *Acipenser gueldenstaedtii*, cleared and stained series (VIMS 33601), showing head in ventral view, anterior facing left. (a) 14 mm TL, scale is 1 mm. (b) 16.8 mm TL, scale is 1 mm. (c) 19.8 mm TL, scale is 1 mm. (d) 20.5 mm TL, scale is 1 mm. (e) 31 mm TL, scale is 2 mm. (f) 101 mm TL, scale is 5 mm. Abbreviations: br, branchiostegal; cb, ceratobranchial; cd, notochord; cha, anterior ceratohyal; chp, posterior ceratohyal; cl, cleithrum; clv, clavicle; d(t), toothed dentary; dpl(t), toothed dermopalatine; e, eye; gf, gill filaments; iclv, interclavicle; j, jugal; llc, lateral line canal; lrb, lateral rostral canal bone; mc, Meckel's cartilage; pfs, "pectoral fin spine"; pq, palatoquadrate; scc, scapulocoracoid cartilage; so, subopercle; tc, *trabecula cranii*; vrb, ventral rostral bones; *, prootic incisure

3.2.3 | 19.8 mm TL (Figures 5c, 6c, and 7c)

The neurocranium is well formed and the rostroethmoidal, orbital, otic, and occipital regions are all distinct. The rostrum is a strong, massive block of cartilage. Its anterior edge is blunt and broadly rounded with small notches where the sensory canals of the ventral side pierce and the lateral rostral canal bones form (Figure 6c). The sides of the rostrum extend posterolaterally to join the nasal capsule. In the dorsal midline large fontanelles persist in the roof of the neurocranium. At the level of the posterior nasal wall, a cartilaginous bridge reaches toward the dorsal midline. Farther posteriorly, the developing epiphyseal bridge is

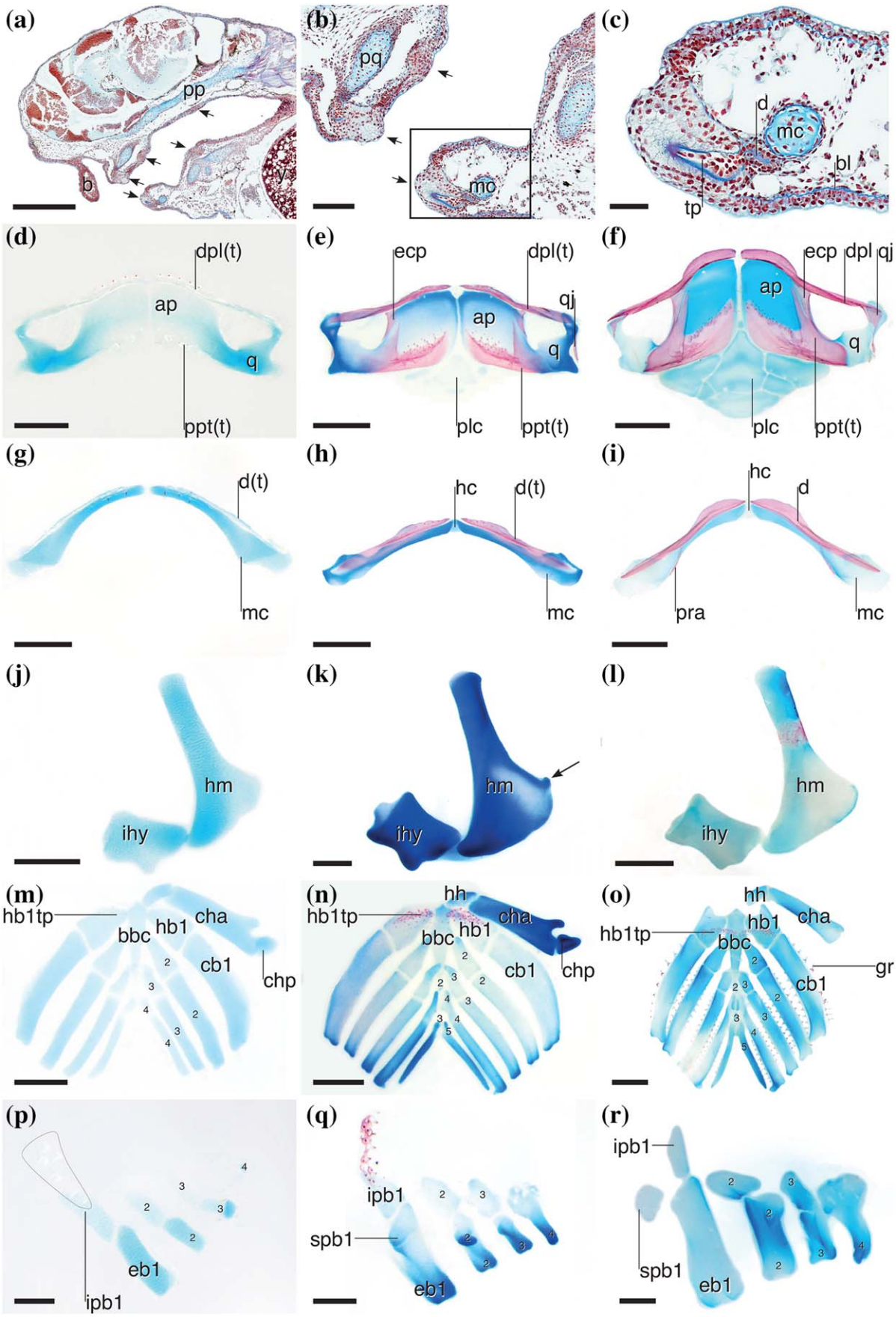
(a)
pp
b
y
(b)
pq
mc
(c)
d
mc
bl
tp
(d)
dpl(t)
ap
q
ppt(t)
(e)
ecp
dpl(t)
qj
ap
q
plc
ppt(t)
(f)
ecp
dpl
qj
ap
q
plc
ppt(t)
(g)
d(t)
mc
(h)
hc
d(t)
mc
(i)
hc
d
pra
mc
(j)
hm
ihy
(k)
hm
ihy
(l)
hm
ihy
(m)
hb1tp
bbc
hb1
cha
cb1
chp
(n)
hh
hb1tp
cha
bbc
hb1
cb1
chp
(o)
hh
hb1
cha
hb1tp
bbc
gr
cb1
(p)
eb1
ipb1
(q)
ipb1
spb1
eb1
(r)
ipb1
spb1
eb1

FIGURE 8.

present at the anterior border of the otic region and the *tectum synoticum* in its medial part. Anterior to the *tectum synoticum*, a large fontanelle persists and extends to the orbital region to join the pineal fontanelle, restricted only by the developing epiphyseal bridge. Posterior to the *tectum synoticum* another smaller fontanelle is present in the occipital region. The occipital arches meet in the midline at the very posterior extent of the neurocranium to form a moderate crest with a small hook- like, posteriorly directed process. From the dorsolateral portion of the occiput, a small posttemporal process projects posterolaterally. The scleral cartilage surrounds most of the eyeball. The barbels insert on the ventral side of the rostrum anterior to the nasal capsule.

The dentary, the dermopalatine, and palatopterygoid, together with their associated teeth, are more strongly developed than in the previous stage. The posteroventral part of the hyomandibula is further enlarged to form the ventral hyomandibular cartilaginous blade. The branchial arch elements decrease in size from anterior to posterior. The hypobranchial and parasphenoid tooth plates on the ventral and dorsal surface of the branchial chamber are more pronounced. Ceratobranchial 5 is the sole element of the fifth gill arch. Epibranchials 1 to 4 are present. Infrapharyngobranchials 1 to 3 and suprapharyngobranchials 1 and 2 are present and attach the gill arches to the neurocranium.

A thin subopercle is present in the skin flap covering the gill cavity and the first dorsal scute is weakly developed (Figure 5c). In some specimens of a similar stage, a dermopterotic is also present.

3.2.4 | 20.5 mm TL (Figures 5d, 6d, and 7d)

At this stage, the dermal skull elements become more apparent and overlie the neurocranium. The rostrum elongates moderately and is more pointed anteriorly compared to previous stages, resulting in a less steep head profile. Chondrification of the neurocranial roof has advanced toward the midline, and the posterior fontanelle is closed in the occipital region. The anterior fontanelle is separated from the pineal fontanelle by the closure of the epiphyseal bridge. The scleral cartilage is now forming a rounded capsule.

In the upper jaw, a quadratojugal is formed (see Figure 8e for position in larger specimen). The tooth bearing elements of the jaws (Figure 7d) and the gill cavity have advanced in development. The teeth on the dentary, dermopalatine, and palatopterygoid, as well as those on the parasphenoid and hypobranchial tooth plates are longer and more pronounced than compared to the smaller stages. The parasphenoid tooth plate in the dorsal gill cavity is now supported by the parasphenoid medially. The parasphenoid is weakly developed at this stage and present as a thin elongate ossification along the base of the neurocranium.

The first elements of the dermatocranium are weakly developed as direct ossifications. The lateral rostral canal bone forms around the sensory canal at the anterior tip of the rostrum (Figure 6d). The frontal and dermopterotic are present although the former is weakly developed above the eye. The dermopterotic and parietal are formed posteriorly at the level of the hyomandibula. The dermopterotic is a thin rod-like structure and the parietal is more plate-like and bears a crest posteriorly. A single small branchiostegal is present ventral to the subopercle. The dorsal scutes are now thin calcified plates in the dorsal finfold and more prominent than at earlier stages (Figure 5d).

The pectoral girdle is connected to the neurocranium by the posttemporal and the supracleithrum, which attach to the posttemporal process. Ventrally, a suprascapular cartilage starts to form. The scapulocoracoid cartilage is further supported by the clavicle and the cleithrum (Figure 7d). The propterygium is extended anteriorly.

3.2.5 | 31 mm TL (Figures 5e, 6e, 7e, and 8e,h,k,n,q)

The dorsal roof of the neurocranium is closed and large parts of it are covered by dermal elements.

The two rami of Meckel's cartilage are joined by a mass of hyaline cartilage in the midline anteriorly (Figure 8h). The teeth associated with the dentary and the dermopalatine are less prominent than in earlier stages and their bases are incorporated into the bones. The tooth field on the palatopterygoid no longer extends to the posterior edge, but is restricted to the anteromedial part, where teeth remain prominent. Lateral to the series of teeth, the palatopterygoid extends anteriorly with a pointed process that is in contact with the triangular ectopterygoid. The quadratojugal is small and rod-shaped. Posterior to the juncture between the left and right palatoquadrate cartilages, the palatal complex is present and consists already of five distinct cartilages (Figure 8e). The anterior surface of the interhyal fills the space between the jaw articulation and the ventrolateral process of the *pars quadrata* of the palatoquadrate cartilage. On the dorsoposterior edge of the ventral hyomandibular cartilaginous blade, a small process is present at this

FIGURE 8 Detailed views on histological sections of *Acipenser baerii* (uncatalogued) and dissected specimens of *A. gueldenstaedtii* (VIMS 33601) highlighting elements of mandibular, hyoid and gill arches. (a) parasagittal section of head, arrows indicating thickening of epithelium at site of tooth development, scale is 0.5 mm. (b) detail of same section, scale is 0.25 mm. (c) detail of same section, scale is 0.1 mm. (d) 16.8 mm TL upper jaw in ventral view, scale is 0.5 mm. (e) 31 mm TL upper jaw in ventral view, scale is 1 mm. (f) 101 mm TL upper jaw in ventral view, scale is 2 mm. (g) 16.8 mm TL lower jaw in dorsal view, scale is 0.5 mm. (h) 31 mm TL lower jaw in dorsal view, scale is 1 mm. (i) 101 mm TL lower jaw in dorsal view, scale is 2 mm. (j) 16.8 mm TL hyomandibula in lateral view, scale is 0.5 mm. (k) 31 mm TL hyomandibula in lateral view, scale is 0.5 mm, arrow points out small process. (l) 101 mm TL hyomandibula in lateral view, scale is 2 mm. (m) 16.8 mm TL ventral gill arches in dorsal view, scale is 0.5 mm. (n) 31 mm TL ventral gill arches in dorsal view, scale is 1 mm. (o) 101 mm TL ventral gill arches in dorsal view, scale is 0.5 mm. (p) 16.8 mm TL dorsal gill arches in dorsal view, scale is 0.25 mm, drawn line indicates extension of toothplate. (q) 31 mm TL dorsal gill arches in dorsal view, scale is 0.5 mm. (r) 101 mm TL, dorsal gill arches in dorsal view, scale is 1 mm. Abbreviations: ap, *pars autopalatina* of palatoquadrate cartilage; b, barbel; bbc, basibranchial copula; bl, basal lamina; cb, ceratobranchial; cha, anterior ceratohyal; chp, posterior ceratohyal; d, dentary; d(t), toothed dentary; dpl, dermopalatine; dpl(t), toothed dermopalatine; eb, epibranchial; ecp, ectopterygoid; gr, gillraker; hb, hypobranchial; hb1tp, toothplate on hypobranchial 1; hc, hyaline cartilage; hh, hypohyal; hm, hyomandibula; ihy, interhyal; ipb, infrapharyngobranchial; mc, Meckel's cartilage; plc, palatal complex; pp, parachordal plate; ppt(t), toothed palatopterygoid; pra, prearticular; pq, palatoquadrate; q, *pars quadrata* of palatoquadrate cartilage; qj, quadratojugal; spb, suprapharyngobranchial; tp, tooth papilla

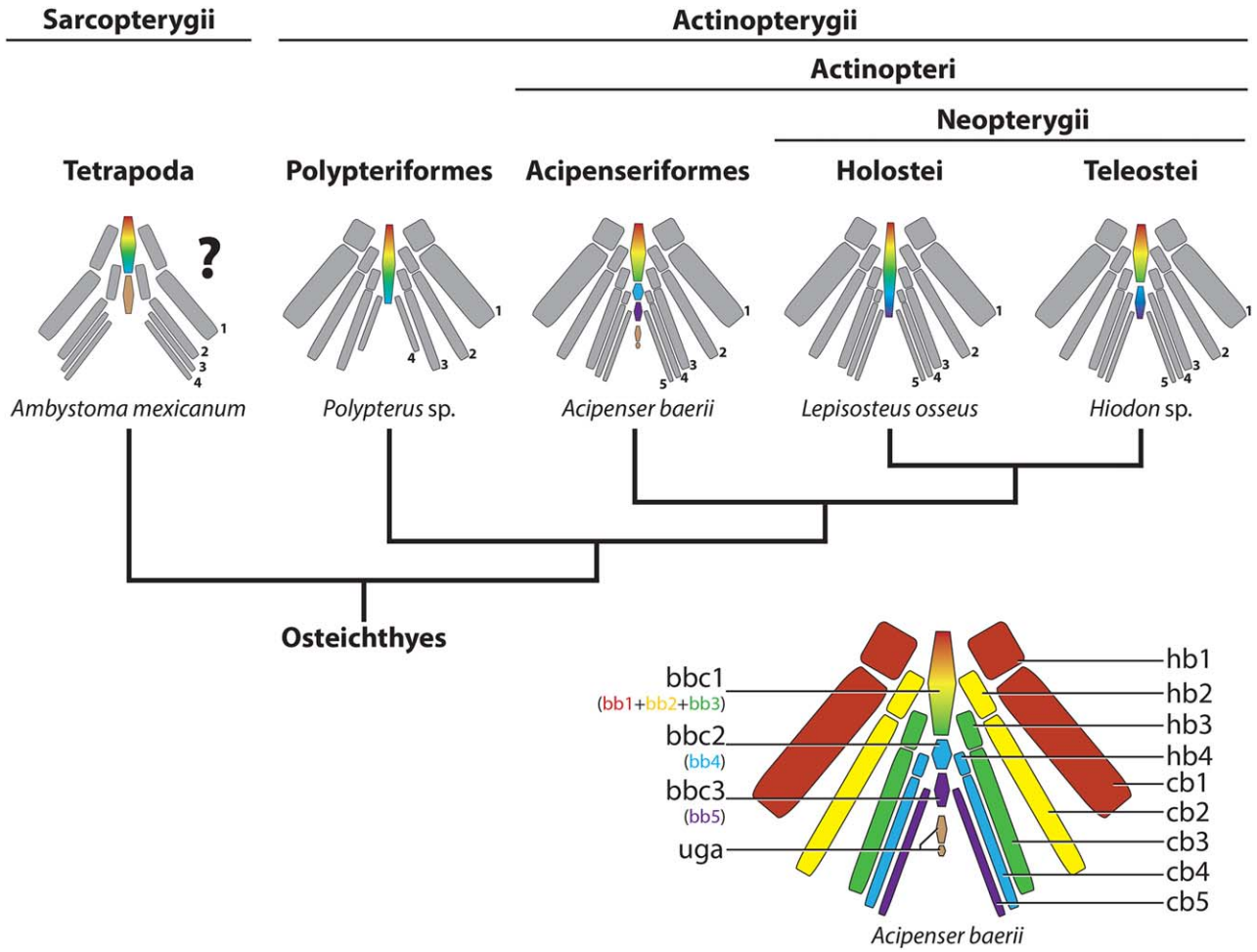

FIGURE 9 Schematic view of the ventral gill-arch skeleton of different osteichthyan taxa, paired skeletal elements colored in gray and numbered in an anteroposterior sequence, median unpaired cartilages colored in correspondence to the associated branchial arch (red, first branchial arch (BA); yellow, second BA; green, third BA; blue, fourth BA; violet, fifth BA, unidentified gill-arch elements and basibranchial 2 of *Ambystoma mexicanum* colored in light brown, question mark indicates lack of information on the developmental timing. Abbreviations: bb, basibranchial; bbc, basibranchial copula; cb, ceratobranchial; hb, hypobranchial; uga, unidentified gill-arch element

stage (Figure 8k). The other elements of the hyoid arch are similar to those described in the previous stage. Posterior to the large anterior basibranchial copula two small additional basibranchial copulae are present at the anterior tips of ceratobranchials 4 and 5. Hypobranchial 1 has a broad proximal part that fits in a groove of the anterior basibranchial copula. Hypobranchial 3 extends under the anterior basibranchial copula by a ventromedial process. Hypobranchials 1 to 3 are distinct from the ceratobranchials. In the fourth gill arch, such a separation is indicated but not clearly present. Ceratobranchial 1, which bears six weakly developed anterior gill rakers, is significantly more massive than the slender more posterior ceratobranchials. A small posteriorly directed process is present on the distal tip of ceratobranchial 4 (Figure 8n). The club-shaped epibranchial 4 is larger than epibranchial 3. Infrapharyngobranchial 1 inserts on the posterior side of the ascending ramus of the parasphenoid and the small suprapharyngobranchial 1 articulates with the braincase posterolaterally. Suprapharyngobranchial 2 is about twice the length of suprapharyngobranchial 1 and articulates with the otic region of the braincase (Figure 8q).

The first dorsal (Figure 5e) and ventral rostral (Figure 7e) bones are present at the tip of the rostrum and bear thorn-like crests. Behind the nasal opening a small nasal lies isolated from the other dermal bones. The frontal is larger in size than in the previous stage and forms a crested plate anterior to the parietal, which has a rough surface consisting of thorn-like protuberances. Between the parietals and anterior to the first dorsal scute, a weakly developed median extrascapular forms around the supratemporal sensory canal (Figure 6e). Lateral to the frontal and dorsoposterior to the eye, a triangular dermosphenotic is now present. Ventral to the dermosphenotic and separated by a gap, a thin postorbital defines the posterior margin of the orbital region. The jugal is now present and is triangular in shape, with a rounded posterior and a concave anterior side. The dermopterotic is elongate but broader than in the previous stage. Ventral to the subopercle, which now bears small protuberances, a second branchiostegal is present. The parasphenoid is enlargened and covers the neurocranium ventrally.

The pectoral fin is supported by a short pectoral-fin spine anteriorly and 8–9 fin rays posteriorly (right side of specimen is without

ossified fin rays). In addition to the proximal radials, distal radials are present as well. The cleithrum and the clavicle are much more strongly developed than in the previous stages (Figure 7e).

3.2.6 | 101 mm TL (Figures 5f, 6f, 7f, and 8f,i,l,o,r)

Most of the neurocranium is covered by dermal elements. On its ventral surface, large basitrabecular processes are formed.

On the posterior edge of the bow-shaped Meckel's cartilage the small, rod-like prearticular is formed. No teeth are visible on the dentary, but the bone forms an elevated crest medially where teeth were present at earlier stages (Figure 8i). The ectopterygoid joins the anterior process of the palatopterygoid. The triangular quadratojugal has a posterior extension and covers the dorsolateral part of the *pars quadrata* of the palatoquadrate cartilage. The palatal complex now consists of nine chondrifications (Figure 8f).

The hyomandibula begins to ossify perichondrally as a bony sheath around the shaft (Figure 8l). A small center of ossification is present on the dorsal surface of the anterior ceratohyal. The interhyal is a robust element and forms a socket to articulate with the jaws. The tooth plate on hypobranchial 1 extends on to the anterior basibranchial copula and meets its counterpart in the midline. The parasphenoid tooth plate is reduced to a few isolated teeth in the epithelium. Ceratobranchials 1–5 bear gill rakers (Figure 8o).

Additional dorsal rostral bones are present and expanded to fully cover the medial part of the rostrum (Figure 6f). Lateral rostral bones are now present but well separated from the dorsal rostral bones by ampullary fields. The ventral rostral bones are restricted to the midline. The rostral sensory canal on the ventral side of the rostrum is supported by a series of rostral canal bones. This canal extends posterolaterally from the lateral rostral canal bones to curve laterally around the barbels before joining the posteroventral corner of the jugal (Figure 7f). From there, it extends through the postorbital to the dermosphenotic where it splits into the supraorbital canal anteriorly and the otic canal posteriorly (Figure 5f). The supraorbital sensory canal runs through the frontal and nasal and is extended anteriorly by a tubular bone in front of the nasal. The otic sensory canal reaches posteriorly from the dermosphenotic and continues into the dermopterotic.

The nasal is larger than in previous stages and contacts the frontal posteriorly and to the supraorbital laterally. In this specimen the dermosphenotic and dermopterotic have fused to form a large bone lateral to the parietal. The parietal now extends to the middle of the eye anteriorly and its unornamented posterior extension is covered by the extrascapulars and the first dorsal scute at the height of the posttemporal. The frontals and parietals of the left and the right sides are not in contact in the midline. Posteriorly, the parietals are separated by a median extrascapular which carries the sensory canal. The subopercle is triangular in shape with a serrated, convex posterior margin and has small protuberances and a crest on its surface. Anteroventally, several small dermal ossifications ornament the cheek between the subopercle and the postorbital (Figure 5f). The specimen illustrated and described has two branchiostegals on the left and three on the right side (Figures 5f and 7f).

The bony elements of the pectoral girdle are more massive. The pectoral-fin spine is elongated and strong. An interclavicle lies dorsal to the clavicles in the midline (Figure 7f) and a postcleithrum is positioned below the posterodorsal part of the supracleithrum.

4 | DISCUSSION

Several ossifications known to be present in sturgeons are not discussed here, as they develop late (e.g., post maturation, see Hilton & Bemis, 1999) and were therefore not present in our specimens. The lacking ossifications of the neurocranium (orbitosphenoid, opisthotic, pterotic, epiotic), of the visceral skeleton (autopalatine, hypohyal, ceratohyal, ceratobranchials, epibranchials, infrapharyngobranchials), and the shoulder girdle (coracoid, scapula, ossifications of the propterygium, metapterygium, and proximal radials) remain to be described for large adults for these species.

We found the early skeletal development of the two species to be similar, with both showing an obvious pattern of developmental sequence. The neurocranium, viscerocranium, and dermatocranium develop as independent entities. The skeleton of sturgeons, generally, although differs in many ways from the condition found in other actinopterygians, and several elements are difficult to homologize. Herein, we follow the terminology of Hilton et al. (2011) to prevent further confusion concerning the naming of individual elements among acipenserids. However, we discuss the homology of certain elements and complexes in the light of our ontogenetic data—specifically the "antorbitals," "basibranchials," and the elements of the hyoid arch. This discussion also highlights the need to further investigate the early skeletal ontogeny of basal actinopterygian fishes, as well as other groups of osteichthyans to achieve a comparative data set.

4.1 | Neurocranium

In both species, the neurocranium follows the general pattern of development found in other craniates (de Beer, 1937). The first neurocranial elements to appear in both species are the parachordals, the *trabecula cranii*, the otic capsule, the orbital cartilage, and the nasal capsule, which fuse during subsequent development to form the neurocranium that encapsules the brain and the sensory organs. Based on our time series of *A. baerii*, the first detectable elements are the otic capsule, which are followed by the precursor of the *trabecula cranii* (Figure 4a). Our identification of the *trabecula cranii* and the otic capsule is based on their position anterior to and dorsolateral to the notochord, respectively. Although our series of *A. gueldenstaedtii* shows the same initial chondrifications as in *A. baerii*, we cannot comment on the sequential timing of the otic capsule and *trabecula cranii* (Figure 5a). Sewertzoff (1928), in his detailed account on the development of *A. ruthenus*, found the anterior tip of the parachordals chondrified at a stage where he could not find any trace of the otic capsule and only a mesenchymatic anlage of the *trabecula cranii*. This development is followed by the fusion of the *trabecula* and the parachordals (Figure 4b) which is corroborated by data of other species of *Acipenser* (de Beer, 1925 studying *A. stellatus*; Holmgren & Stensiö, 1936 studying mainly *A.*

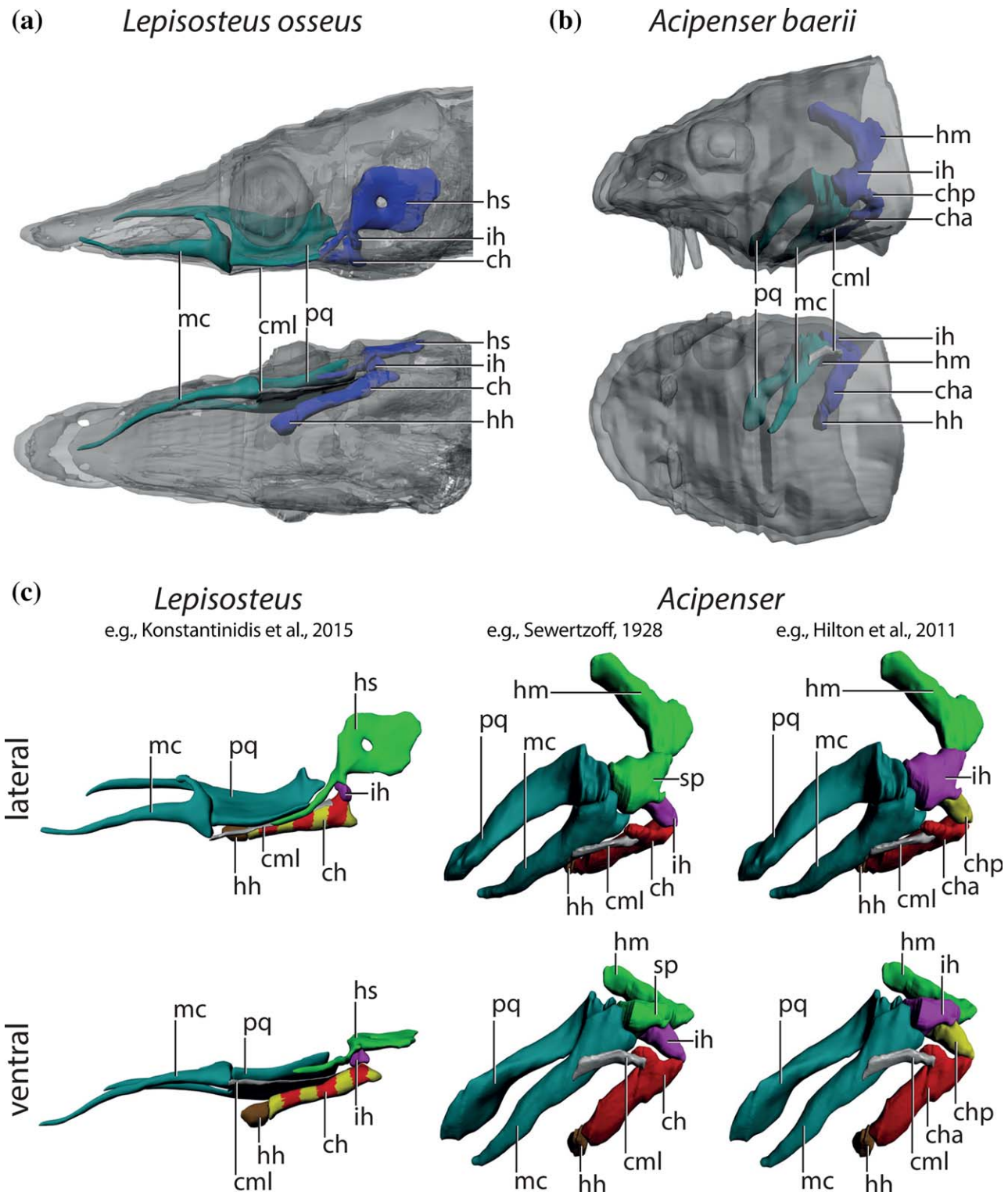

FIGURE 10 Schematic 3D-reconstructions of mandibular and hyoid arch cartilages of *Lepisosteus osseus* and *Acipenser baerii*. (a, b) lateral and ventral view of the mandibular and hyoid cartilages of *L. osseus* (a) and *A. baerii* (b), elements of the mandibular arch are colored in light blue and elements of the hyoid arch in dark blue. (c) different interpretations of the hyoid arch elements of *Acipenser* compared to *Lepisosteus*, mandibular arch is colored in light blue, hyoid arch elements regarded as homologous by the different authors are depicted in corresponding colors. Abbreviations: ch, ceratohyal; cha, anterior ceratohyal; chp, posterior ceratohyal; cml, ceratomandibular ligament; hh, hypohyal; hm, hyomandibula; hy, hyosymplectic cartilage; ih, interhyal; mc, Meckel's cartilage; pq, palatoquadrate; sp, symplectic

gueldenstaedtii). Furthermore, the early fusion of the *trabecula* and the parachordals appears to be an actinopterygian character (or perhaps more broadly among gnathostomes) because it is also described for *Polypterus senegalus* (Moy-Thomas, 1933), *Amia calva*, *Lepisosteus* sp., and *Salmo* sp. (de Beer, 1937). However, the early appearance of the otic capsule in *A. gueldenstaedtii* and *A. baerii* seems unusual and has not been found in other species known so far.

Individual structures of the neurocranium that form early are difficult to identify and disagreement about their homology and terminology is widespread. One such case relates to the polar cartilages, which have been identified for a variety of vertebrate taxa. In sturgeons, they have been described as being fused to the parachordals from early on (de Beer, 1937; Sewertzoff, 1928). A recent paper by Kuratani, Adachi, Wada, Oisi, and Sugahara (2013) discussed those elements as the posterior part of the *trabeculae* and hypothesized, that the identification of independent "polar cartilages" is an artifact caused by the reconstruction from histological sections used in earlier works. We did not observe separate polar cartilages in *A. gueldenstaedtii* or *A. baerii* and interpret the structures identified as such by earlier workers as projections of the parachordals. This further corroborates Kuratani et al.'s hypothesis that polar cartilages are artifacts.

We note that Holmgren and Stensiö (1936) label the commissure of the posterior nasal wall directly anterior to the eye as epiphyseal bridge, while Hilton et al. (2011) refer to a structure more posterior as such which is unlabeled by the former authors. Both hypotheses are depicted in Figure 1c. Based on the identification of the epiphysis in our serial sections and virtual sections obtained by confocal laser scanning microscopy of cleared whole mount specimens, we find that Holmgren and Stensiö (1936) correctly labeled the cartilaginous bridge dorsal to the epiphysis.

4.2 | Viscerocranium

The visceral skeleton follows the general craniate development in both species and develops in anteroposterior and ventrodorsal direction (see de Beer, 1937 for a summary of older literature, and e.g., Gillis, Dahn, & Shubin, 2009; Gillis, Modrell, & Baker, 2012; Langille & Hall, 1987 for more recent examples). However, the hypobranchial and ceratobranchial of the first branchial arch are more massive and further advanced than the hyoid arch in specimens between 12-14mm TL. At this stage, larvae rely solely on yolk sac nutrition and the hyoid arch appears not to be functional. However, larvae at this stage are actively swimming and have high oxygen demand that would relate to more pronounced gill-arch elements: In this specific case, the ceratobranchial cartilage 1, which carries gill filaments already in early stages. The appearance of the ventral gill-arch elements prior to the dorsal gill-arch elements could be explained in a similar fashion. Ontogenetically, the primary function for the gill arches is respiration, and secondarily they serve for food processing. Hypobranchial 1 is massive and has an anterior extension in acipenserids, which serves as a counterpart to the palatal complex in food processing (Findeis, 1997). In zebrafish, heterochrony is known in the development of the viscerocranium as well. There, the hyoid arch and the fifth gill arch are advanced in respect to the other arches at some developmental stages (Cubbage & Mabee, 1996), which differs from other teleostean fishes (Langille & Hall, 1987). This heterochrony in *Danio* is most likely linked to the hypertrophy of ceratobranchial 5 due to its involvement in food processing during later stages.

4.3 | Basibranchial copulae and unidentified gill-arch elements

We follow Nelson (1969), who referred to a basibranchial as the median part of the skeleton of each gill arch. This implies that basibranchial 2 is the serial homologue of basibranchial 1, the former being an element of the second gill arch and the latter of the first gill arch. A basibranchial copula in this terminology is an independent element that may contain several basibranchials. In the following discussion, when referring to other authors with different usage, the terms will be set in quotation marks.

We found a variable number of up to five median cartilages in the viscerocranium (Figure 4o), which may be mistaken as five basibranchials due to the implied one-to-one relationship between these and the gill arches. Nevertheless, we interpret these cartilages as (up to) three basibranchial copulae and (up to) two unidentified gill-arch elements (sensu Grande & Bemis, 1991). Furthermore, the anterior basibranchial copula contains basibranchials 1–3 and the second and third basibranchial copulae represent basibranchials 4 and 5, respectively (Figure 9). This condition is typical for acipenseriforms (Grande & Bemis, 1991; Hilton et al., 2011; Nelson, 1969). The anterior basibranchial copula of *A. baerii* and *A. gueldenstaedtii* appears simultaneously with the elements of the hyoid and first branchial arch (Figures 3a and 6a). It elongates posteriorly as hypobranchials 2 and 3 appear (Figures 4m and 8m). The posterior basibranchial copulae are much smaller when present and relate to gill arches four and five (Figures 4o and 8n, o). Their presence is variable in *A. baerii* and *A. gueldenstaedtii*, even in specimens of similar ontogenetic stage, a phenomenon previously described and discussed for *A. brevirostrum* (Hilton et al., 2011). The position of the unidentified gill-arch elements posterior to the rest of the viscerocranium and the independent developmental timing of these elements in *A. baerii* and *A. gueldenstaedtii* supports the hypothesis of an independent developmental and evolutionary origin. They are the only elements of the branchial skeleton that appear after yolk sac consumption, and much later than all other viscerocranial elements. In some amphibian model species, such as *Ambystoma mexicanum*, two median cartilaginous elements are present in the viscerocranium. The anterior, commonly termed "basibranchial 1," as most of the viscerocranium, is formed by neural crest (Olsson, Falck, Lopez, Cobb, & Hanken, 2001). Stone (1926), based on an extirpation experiment in *Ambystoma*, and Olsson et al. (2001) based on a fate mapping experiment in *Bombina* found that what is usually referred to as "basibranchial 2" is not of neural crest origin. More recently in *Ambystoma*, Davidian and Malashichev (2013) and Sefton, Piekarski, and Hanken (2015) showed that in this taxon, "basibranchial 2" is of mesodermal origin. The lack of lineage tracing data in basal actinopterygians to date impedes an evolutionary interpretation of the data presented herein, but it gives a possible

explanation for the unidentified gill-arch elements in sturgeons, even though it is unlikely these structures are homologous with their counterparts in amphibians.

The homology and evolution of median branchial arch elements among osteognathostomes has been discussed extensively (Gardiner, 1973; Nelson, 1969; Wiley, 1976). For actinopterygians, a single basibranchial copula has been considered the ancestral condition that can be observed in polypteriforms (Gardiner, 1973), the most basal extant actinopterygian taxon. In extant polypteriforms, the hyoid arch and gill arches articulate with a single basibranchial copula (Allis, 1922; Daget, Bauchot, Bauchot, & Arnoult, 1964; Jollie, 1984). However, polypteriforms are highly derived, as they have only four gill arches and the most posterior gill arch is represented by a ceratobranchial only (Britz & Johnson, 2003). Phylogenetically, Acipenseriformes are positioned between Polypteriformes and the Neopterygii, the latter comprising the Holostei (Lepisosteiformes and Amiiformes) and their sister taxon Teleostei (Betancur-R et al., 2013; Grande, 2010). For *Lepisosteus platystomus* (Neopterygii, Lepisosteiformes), Hammarberg (1937) described a single basibranchial copula extending from the basihyal to the fifth gill arch in developmental stages from 16 mm up to 65.4 mm. Grande (2010) found two independent, mostly cartilaginous "basibranchials" (basibranchial copulae *sensu* Nelson, 1969) in specimens of *L. osseus* from 153 mm SL on. One short "basibranchial 1," connecting the hyoid arch with the first branchial arch and an elongate "basibranchial 2" to which gill arches 2-5 attach. A single small ossification is present in the anterior portion of the posterior "basibranchial." Teleostean fishes have up to three independent copulae: a basihyal and two basibranchial copulae (Nelson, 1969). The anterior basibranchial copula supports three ossifications, matching the number of paired gill-arch elements with which they are associated. The posterior basibranchial copula does not ossify and is referred to as basibranchial 4-5 or 4-6 (Nelson, 1969). The latter interpretation is based on its elongation beyond the fifth gill arch in some taxa, similar to the unidentified gill-arch elements in sturgeons. A phyletic trend, as discussed by Nelson (1969) is not easy to draw from this, but it seems that a multiplication or subdivision of ancestrally single elements took place in the evolution of the actinopterygian median gill-arch elements. This, however, implies that any attempt to number basibranchials simply by the number of hypobranchial/ceratobranchials associated with them does not necessarily reflect homology.

4.4 | Hyoid arch

The hyoid arch of acipenseriforms is unique among extant actinopterygians because it develops from five separate cartilages, with three cartilages below the jaw joint. To homologize these elements across actinopterygians is difficult because of the mismatch in numbers of elements across taxa between acipenseriforms and neopterygians (see Figure 10). While there is little doubt concerning the identity of the terminal elements of the series, the hyomandibula and the hypohyal, respectively, the three intercalated cartilages have been identified variably. One interpretation is that the acipenseriform interhyal and hyomandibula correspond to the neopterygian hyosymplectic and the elements of the acipenseriform hyoid arch were named "symplectic," "interhyal," and "ceratohyal" (e.g., de Beer, 1937; Sewertzoff, 1928; Stengel, 1962; van Wijhe, 1882). Patterson (1982) argued, that (i) the acipenseriform "interhyal" is a posterior ceratohyal, as it carries a branchiostegal ray in *Polyodon* (McAllister, 1968; van Wijhe, 1882) and (ii) by comparing the hyoid arch of extant acipenseriforms with the fossil †*Pteronisculus*. Grande and Bemis (1991) further established this terminology, mainly following the argument of the close articulation of the branchiostegal bone with the posterior ceratohyal in *Polyodon*. However, branchiostegal rays can be associated with other elements than the ceratohyal, as exemplified by some stomiiform teleosts (McAllister, 1968). Regardless of this, the terminology has since then been applied on the fossils †*Pteronisculus*, †*Boreosomus*, and †*Pycholepis* (Gardiner, Maisey, & Littlewood, 1996) as well as other fossil and extant acipenseriforms (Findeis, 1997 and many others). This interpretation implies that the presence of an anterior and a posterior ceratohyal is a synapomorphy of Actinopteri instead of the Neopterygii (Nelson, 1969) and that the symplectic is a neopterygian character.

The development of some of these elements in neopterygians is different from that seen in *Acipenser*. The anterior and posterior ceratohyal occur as independent ossifications within a single cartilage in *Lepisosteus* (Hammarberg, 1937), *Amia* (Grande & Bemis, 1998), and teleosts (e.g., Hilton, 2002a; see also van Wijhe, 1882) and thereby differ from the two independent cartilages found in sturgeons. Similarly, the symplectic and the hyomandibula form as ossifications from a common cartilaginous progenitor (hyosymplectic cartilage) in neopterygians (Pehrson, 1922). The development of these elements is therefore different between acipenseriforms and neopterygians, complicating the homology statements. This difference is further exemplified by the fact that the hypohyal of teleosts develops two centers of ossification as well. The hyoid arch elements in fossil and extant chondrosteans were labeled as the "symplectique," "interhyal," and "neoceratohyale" by Véran (1988). She justified this terminology with embryological evidence for a "symplectique" (interhyal) in the works of Parker (1881), de Beer (1925), and Sewertzoff (1928), stating that especially the latter found two centers of chondrification in one cartilage that separate later in development. Sewertzoff (1928) however describes tissue that has "not yet differentiated" in the region of the "symplecticum and stylohyale," while the hyomandibula was already starting to chondrify and that later, when the "symplecticum" starts to chondrify, this portion is connected with the hyomandibula by procartilage, while it is clearly separated from the ventral "stylohyal" (posterior ceratohyal). We however never observed the interhyal to be connected with the hyomandibula. We can confirm that the latter is slightly advanced in its state of chondrification with respect to the interhyal and posterior ceratohyal in early developmental stages around 8.5 mm SL in *A. baerii* and *A. gueldenstaedtii*. If Sewertzoff (1928) was right, and the interhyal and hyomandibula of acipenseriforms form from one piece, their development still is different from neopterygians as described above. Hence, there is no embryological evidence for a "symplecticum" in chondrosteans.

In contrast, an argument against the current (Findeis, 1997; Grande & Bemis, 1991; Hilton et al., 2011; Patterson, 1982) terminology and

homologization is the connection of the hyoid and mandibular arches by the ceratomandibular ligament. It consistently connects Meckel's cartilage to the posterior ceratohyal in neopterygians (Konstantinidis et al., 2015; Lauder, 1980; van Wijhe, 1882; Wiley, 1976). In acipenseriforms, it attaches to the anterior ceratohyal as can be seen by a strong process that serves as its attachment site (Figure 4n). The homology of the posterior ceratohyal is therefore doubtful and if the element ventral to the hyomandibula is not a symplectic, but a hypertrophied interhyal as currently agreed on, a surplus element is present in acipenserids. The homology of the hyoid arch elements in acipenserids is therefore far from "clarified" as stated by Gardiner, Schaeffer, and Masserie (2005) and requires further investigation.

4.5 | Lateral rostral canal bone and antorbitals

The lateral rostral canal bone of sturgeons has been homologized with the antorbital of other actinopterygians, as it is the anteriormost paired bone surrounding the infraorbital sensory canal (Allis, 1905); no rostral is present. Its far anterior position with respect to the eye raised doubts on this homology statement (Jollie, 1980), although that can be explained by the unique shape of the head in sturgeons (i.e., it is positioned anteriorly as a consequence of rostrum elongation and the posteroventral positioning of the mouth). The antorbital of Allis (1905), however, should not be confused with the antorbital of Findeis (1997) and Bemis et al. (1997), which is here termed the supraorbital, as discussed in Hilton (2002b). Hilton (2002b) considered evidence for Allis' (1905) homologization in the specific shape of the lateral rostral canal bone (triradiate, sensory canal bearing) and similarly shaped antorbitals in the stem acipenseriforms †*Peipiaosteus pani* (Grande & Bemis, 1996; Zhou, 1992;) and †*Chondrosteus acipenseroides* (Grande & Bemis, 1996); Hilton and Forey (2009) however could not find such a bone in †*C. acipenseroides*, but stated that this might be due to lack of preservation.

The lateral rostral canal bone, at the most anterior tip of the rostrum, ossifies as the very first element of the skull in *A. baerii* (Figure 1c) and *A. gueldenstaedtii* (Figure 5c), followed by the tooth bearing elements (dentary, palatopterygoid, dermopalatine). Most other dermatocranial elements appear in a posterior to anterior direction and start posterolaterally after the aforementioned elements. The anamestic rostral bones are the last elements to ossify and form in an anterior to posterior direction. The lateral rostral canal bone therefore is very different from its surrounding elements in its timing of development. This characteristic early formation provides further evidence for its homology with the antorbital of other actinopterygians. In *Polypterus* (Jollie, 1984; Pehrson, 1947), *Lepisosteus* (Hammarberg, 1937) and *Amia* (Pehrson, 1922), the bones associated with the infraorbital sensory canal form in anteroposterior direction. The multiple lacrimal bones surrounding the infraorbital sensory canal in lepisosteids develop as a single anlage and appear earlier (18.7 mm) than the antorbital in *Lepisosteus platostomus* (33.4 mm) and much earlier than other bones of the infraorbital sensory canal such as the infraorbital and dermosphenotic (both at 65.4 mm; Hammarberg, 1937).

The lateral rostral canal bone of sturgeons therefore corresponds to the antorbital of other actinopterygians in its position, its formation around the infraorbital sensory canal, as well as in its shape and developmental sequence and therefore has to be considered homologous.

4.6 | Dentition

Adult sturgeons are edentulous while larval stages have teeth associated with the jaws and gill-arch elements. Teeth are formed and later become nonfunctional in an anteroposterior direction. We found teeth to form in a thickening of the epithelium in direct vicinity of the bones of the upper and lower jaw and subsequently in the gill cavity. Within the thickening of the epithelium, a pulp cavity is formed and the mineralization of the teeth starts distally (Figure 8a–c). Later, teeth become completely ankylosed to the underlying bone. This is also the case in *Polyodon spathula* (Georgi & Brady, 1999) and is typical for actinopterygians generally (Fink, 1981).

Bemis et al. (1997) described this mode of tooth formation for *Polyodon spathula* but stated that a different mode was generally accepted for *Acipenser* in which they were "shed" during later development. Teeth are lost at different points in development in different species of Acipenseridae (e.g., earlier in *A. brevirostrum*; Hilton et al., 2011) and we found remnants of palatopterygoid teeth in an adult specimen of *Pseudoscaphirhynchus hermanni*. Although further study of tooth formation and loss in Acipenseriformes is warranted, the teeth of sturgeons appear not to be actively reduced or "shed." Instead it seems that the pointed tips wear and break off and, in the case of the teeth associated with the dentary (Figures 4e and 8e) and dermopalatine (Figures 4h and 8h), the bases of the teeth become incorporated into the growing matrix of the bone.

4.7 | Intraspecific and interspecific variation

Where variation in the development of the head skeletons occurred between comparable specimens of the two species, often also intraspecific variation was found. For phylogenetic purposes, it is necessary to separate phylogenetically informative characters from the overall observed intraspecific variation (Grande, 2004; Hilton & Bemis, 1999, 2012). Several of the differences found between *A. baerii* and *A. gueldenstaedtii* are considered variable by other authors and would require a much larger data set and quantitative analysis to infer species-specific characters. For example, the presence/absence of external hyoid arch cartilages is not considered a character and most likely subject to intraspecific variation and life history stage. Similarly, the fusion of the dermopterotic and dermosphenotic has been observed to occur in some taxa and specimens previously (see Hilton et al., 2011 for *A. brevirostrum*). Lateral extrascapulars were observed to occur in some specimens of both species, and sometimes within one individual they can occur on one side only. The parasphenoid was found to develop later in *A. baerii* (first observed at 104 mm TL) than in *A. gueldenstaedtii* (first observed at 21 mm TL) and we were surprised to find such a great range in the onset of development of this bone. We cannot exclude the possibility that this bone was not observed at earlier stages of *A. baerii* due to preparation methods, as the cartilage staining in our

specimens of *A. baerii* is very heavy and may have obscured the staining of a weakly ossified bone.

The most obvious difference between the two species is the longer rostrum of *A. baerii* in comparison to the short, stout rostrum of *A. gueldenstaedtii*. This difference becomes evident at around 20 mm TL and becomes progressively greater from then on, as the rostrum of *A. baerii* keeps growing; this serves as a good character to distinguish the two species. The rostrum of *A. gueldenstaedtii* stays short throughout ontogeny. This is in contrast with *A. brevirostrum*, which has a very elongate rostrum in larval and small juvenile stages, but has a short, rounded snout in subadults and adults (see Hilton et al., 2011). Coding rostrum length in sturgeons as a phylogenetic character, therefore, should include information on life history stage.

Another character that has been used in phylogenetic analyses and may be related to the short rostrum is the length of dorsal rostral bones. As the dorsal rostral bones in our largest specimens are still incompletely developed, we cannot comment on the adult character state. In our specimens the dorsal rostral bones do not appear to be very different in length between *A. baerii* and *A. gueldenstaedtii*. We do, however, see a difference in the dorsal rostral bones regarding the coverage of the rostrum in specimens of the same age and length. In *A. baerii*, the dorsal rostral bones leave the lateral parts of the rostrum in our largest specimen (104 mm TL) uncovered, while in *A. gueldenstaedtii* these parts are at least partly covered in specimens of the same age and size.

The elements of the pectoral girdle and their sequence of ossification have been studied in detail for *Scaphirhynchus albus*, *A. medirostris*, *A. transmontanus*, and *A. fulvescens* by Dillman and Hilton (2015). The supracleithrum was, in all four, the first element to ossify and this pattern is matched for the species examined here. Furthermore, the condition in the species of the genus *Acipenser* used in their study matches our observations for *A. baerii* and *A. gueldenstaedtii* in that the cleithrum develops prior to the clavicle (except for in *A. transmontanus*), and is followed by the interclavicle. The ossification of the posttemporal and postcleithrum varies between the species and occurs at different times. For *A. baerii* and *A. gueldenstaedtii* the complete sequence is as follows: supracleithrum – posttemporal – cleithrum – clavicle – interclavicle – postcleithrum. The highest degree of similarity in the sequence of ossification can be seen between *A. fulvescens*, *A. baerii*, and *A. gueldenstaedtii*, as only the sequence of the posttemporal differs. It develops after the cleithrum and simultaneously with the clavicle in *A. fulvescens* instead of before the cleithrum. *Acipenser baerii* and *A. gueldenstaedtii* are further similar to *S. albus* in their sequence of ossification of the supracleithrum, posttemporal, and cleithrum. The sequence of development of the clavicle, interclavicle, and postcleithrum is unresolved or they appear simultaneous in *S. albus*. *Acipenser transmontanus* differs by an early ossifying clavicle (second to the supracleithrum) and displays simultaneous ossification of the posttemporal and cleithrum. In *A. medirostris*, as in *A. fulvescens*, the cleithrum is the second element to develop. *Acipenser medirostris* further shows heterochronic development of the postcleithrum, as it appears simultaneously with the posttemporal and before the clavicle and interclavicle. Potentially relevant for this taxonomic framework are the sequence shared by *A. baerii*, *A. gueldenstaedtii*, and *S. albus* and the sequence shared by *A. baerii*, *A. gueldenstaedtii*, and *A. fulvescens*, as well as the early ossification of the cleithrum (or delayed ossification of the posttemporal) shared by *A. medirostris* and *A. fulvescens*. The simultaneous appearance of the posttemporal with the cleithrum in *A. transmontanus* can be interpreted as an intermediate character state. *Scaphirhynchus* is possibly sister to all other extant Acipenseridae with a long independent history (Birstein et al., 2002; Hilton et al., 2011). The sequence shared by *S. albus*, *A. baerii*, and *A. gueldenstaedtii* is therefore either convergent or represents a plesiomorphic state that is retained in all three and then derived in the North American species of the genus *Acipenser* analyzed by Dillman and Hilton (2015). The higher degree of similarity between *A. fulvescens*, *A. baerii*, and *A. gueldenstaedtii* fits well with many phylogenetic hypotheses that have more or less closely grouped these species together and separate from *A. medirostris* and *A. transmontanus* (Birstein et al., 2002; Krieger et al., 2008). Further data for more species will be needed to interpret the sequences and to fully exploit their significance for phylogenetics.

5 | CONCLUSIONS

Developmental morphology not only provides information to include in phylogenetic analyses but also provides data on the timing of development and gives insights into the homology of elements. Our data supports a homology of the lateral rostral canal bone of sturgeons and the antorbital of other actinopterygians and that the unidentified gill-arch elements of sturgeons are not basibranchials but that there are three basibranchial copulae in sturgeons that relate to gill arches 1–3, 4, and 5, respectively. We further show that the chondrostean posterior ceratohyal is not homologous with the posterior ceratohyal of neopterygians. Sturgeons are a great model to expand our knowledge on the evolution of vertebrates and as such are an important taxon to study. However, many hypotheses that are raised need further investigation by experimental approaches, such as fate mapping or gene expression analysis. Also, broader comparisons among taxa, both fossil and living, need to be made to understand the level of phylogenetic generality of observations.

ACKNOWLEDGMENTS

We are very thankful to Peter Groß and the hatchery staff at "Fischzucht Rhönforelle" in Gersfeld, Germany for their generous supply of sturgeon eggs. We express special thanks to Christian Schultheiß and Ralf Gensler, who shared their knowledge of sturgeon breeding and raising, and took their time to supply additional material. Katja Felbel was very helpful in the lab and prepared the histological sections. Jörg Hammel assisted with μCT scanning. Robert Cerny gave advice and criticism on an earlier version of this manuscript. Gerta Puchert and Sandra Clemens helped in raising and caretaking of animals. We thank Sarah Huber (VIMS) for curatorial assistance. This is contribution number 3606 of the Virginia Institute of Marine Science, College of William & Mary.

REFERENCES

Allis, E. P. (1905). The latero-sensory canals and related bones in fishes. *Internationale Monatsschrift für Anatomie und Physiologie*, *21*, 401–528.

Allis, E. P. (1922). The cranial anatomy of *Polypterus*, with special reference to *Polypterus bichir*. *Journal of Anatomy*, *56*, 189−294.43.

Bardin, J., Rouget, I., & Cecca, F. (2016). Ontogenetic data analyzed as such in phylogenies. *Systematic Biology*.

Bemis, W., Findeis, E., & Grande, L. (1997). An overview of Acipenseriformes. *Environmental Biology of Fishes*, *48*, 25–71.

Bemis, W. E., & Kynard, B. (1997). Sturgeon rivers: an introduction to acipenseriform biogeography and life history. *Environmental Biology of Fishes*, *48*, 167–183.

Betancur-R, R., Broughton, R. E., Wiley, E. O., Carpenter, K., López, J. A., Li, C., … Ortí, G. (2013). The tree of life and a new classification of bony fishes. *PLoS Currents*, *5*, ecurrents.tol.53ba26640df26640ccaee 26675bb26165c26648c26288.

Birstein, V., & Bemis, W. (1997). How many species are there within the genus *Acipenser*? *Environmental Biology of Fishes*, *48*, 157–163.

Birstein, V. J., & DeSalle, R. (1998). Molecular phylogeny of Acipenserinae. *Molecular Phylogenetics and Evolution*, *9*, 141–155.

Birstein, V. J., Doukakis, P., & DeSalle, R. (2002). Molecular phylogeny of Acipenseridae: Nonmonophyly of Scaphirhynchinae. *Copeia*, *2002*, 287–301.

Birstein, V. J., & Ruban, G. (2004). A comment on the Siberian, *Acipenser baerii*, and Russian, *Acipenser gueldenstaedtii*, sturgeons. *Environmental Biology of Fishes*, *70*, 91–92.

Britz, R., & Johnson, G. D. (2003). On the homology of the posteriormost gill arch in polypterids (Cladistia, Actinopterygii). *Zoological Journal of the Linnean Society*, *138*, 495–503.

Bronzi, P., Rosenthal, H., Arlati, G., & Williot, P. (1999). A brief overview on the status and prospects of sturgeon farming in Western and Central Europe. *Journal of Applied Ichthyology*, *15*, 224–227.

Couly, G. F., Coltey, P. M., & Le Douarin, N. M. (1992). The developmental fate of the cephalic mesoderm in quail-chick chimeras. *Development*, *114*, 1–15.

Couly, G. F., Coltey, P. M., & Le Douarin, N. M. (1993). The triple origin of skull in higher vertebrates: A study in quail-chick chimeras. *Development*, *117*, 409–429.

Cubbage, C. C., & Mabee, P. M. (1996). Development of the cranium and paired fins in the zebrafish *Danio rerio* (Ostariophysi, Cyprinidae). *Journal of Morphology*, *229*, 121–160.

Daget, J., Bauchot, M. L., Bauchot, R., & Arnoult, J. (1964). Développement du chondrocrâne et des arcs aortiques chez *Polypterus senegalus* Cuvier. *Acta Zoologica*, *45*, 201–244.

Davidian, A., & Malashichev, Y. (2013). Dual embryonic origin of the hyobranchial apparatus in the Mexican axolotl (*Ambystoma mexicanum*). *The International Journal of Developmental Biology*, *57*, 821–828.

de Beer, G. R. (1925). Memoirs: Contributions to the development of the skull in sturgeons. *Journal of Cell Science*, *s2-69*, 671–687.

de Beer, G. R. (1937). *The development of the vertebrate skull*. London: Oxford University Press.

de la Herrán, R., Fontana, F., Lanfredi, M., Congiu, L., Leis, M., Rossi, R., … Garrido-Ramos, M. A. (2001). Slow rates of evolution and sequence homogenization in an ancient satellite DNA family of sturgeons. *Molecular Biology and Evolution*, *18*, 432–436.

Dillman, C. B., & Hilton, E. J. (2015). Anatomy and early development of the pectoral girdle, fin, and fin spine of sturgeons (Actinopterygii: Acipenseridae). *Journal of Morphology*, *276*, 241–260.

Dillman, C. B., Wood, R. M., Kuhajda, B. R., Ray, J. M., Salnikov, V. B., & Mayden, R. L. (2007). Molecular systematics of Scaphirhynchinae: an assessment of North american and Central asian freshwater sturgeon species. *Journal of Applied Ichthyology*, *23*, 290–296.

Findeis, E. (1997). Osteology and phylogenetic interrelationships of sturgeons (Acipenseridae). *Environmental Biology of Fishes*, *48*, 73–126.

Fink, W. L. (1981). Ontogeny and phylogeny of tooth attachment modes in actinopterygian fishes. *Journal of Morphology*, *167*, 167–184.

Gans, C., & Northcutt, R. G. (1983). Neural crest and the origin of vertebrates: a new head. *Science*, *220*, 268–273.

Gardiner, B. G. (1973). Interrelationships of teleostomes. In P. H. Greenwood, R. S. Miles, & C. Patterson (Eds.), *Interrelationships of Fishes* (pp. 105–135). Zoological Journal of the Linnean Society.

Gardiner, B. G., Maisey, J. G., & Littlewood, D. T. J. (1996). Chapter 6 - Interrelationships of basal neopterygians. In M. L. J. Stiassny, L. R. Parenti, & G. D. Johnson (Eds.), *Interrelationships of Fishes* (pp. 117–146). Burlington: Academic Press.

Gardiner, B. G., Schaeffer, B., & Masserie, J. A. (2005). A review of the lower actinopterygian phylogeny. *Zoological Journal of the Linnean Society*, *144*, 511–525.

Georgi, T. A., & Brady, D. R. (1999). The teeth of the paddlefish, *Polyodon spathula*. *Journal of Applied Ichthyology*, *15*, 279–280.

Gillis, J. A., Dahn, R. D., & Shubin, N. H. (2009). Shared developmental mechanisms pattern the vertebrate gill arch and paired fin skeletons. *Proceedings of the National Academy of Sciences of the United States of America*, *106*, 5720–5724.

Gillis, J. A., Modrell, M.S., & Baker, C. V. H. (2012). A timeline of pharyngeal endoskeletal condensation and differentiation in the shark, *Scyliorhinus canicula*, and the paddlefish, *Polyodon spathula*. *Journal of Applied Ichthyology*, *28*, 341–345.

Ginsburg, A. S., & Dettlaff, T. A. (1991). The Russian sturgeon *Acipenser gueldenstaedtii*. Part I. Gametes and early development up to time of hatching. In T. A. Dettlaff & S. G. Vassetzky (Eds.), *Animal Species for Developmental Studies* (pp. 15–65). Springer US.

Gisbert, E. (1999). Early development and allometric growth patterns in Siberian sturgeon and their ecological significance. *Journal of Fish Biology*, *54*, 852–862.

Gisbert, E., & Ruban, G. (2003). Ontogenetic behavior of Siberian sturgeon, *Acipenser baerii*: A synthesis between laboratory tests and field data. *Environmental Biology of Fishes*, *67*, 311–319.

Goethe, J. W. V. (1820). Dem Menschen wie den Thieren ist ein Zwischenknochen der obern Kinnlade zuzuschreiben. *Zur Morphologie*, *1*, 199–220.

Grande, L. (2004). Catagorizing types of morphological variation in comparative morphology, and the importance of this to vertebrate paleontology. In G. Arratia & A. Tintori (Eds.), *Mesozoic Fishes 3—Systematics, Paleoenvironments and Biodiversity* (pp. 123–136). München: Dr. Friedrich Pfeil.

Grande, L. (2010). *An empirical synthetic pattern study of gars (Lepisosteiformes) and closely related species, based mostly on skeletal anatomy: The resurrection of Holostei* (Issue 6, i–x, pp. 1–871). Lawrence, Kansas: American Society of Ichthyologists and Herpetologists Special Publication.

Grande, L., & Bemis, W. E. (1991). Osteology and phylogenetic relationships of fossil and recent paddlefishes (Polyodontidae) with comments on the interrelationships of Acipenseriformes. *Society of Vertebrate Paleontology Memoir*, *1*, 1–121.

Grande, L., & Bemis, W. E. (1996). Interrelationships of Acipenseriformes, with comments on "Chondrostei." In M. L. J. Stiassny, L. R. Parenti, & G. D. Johnson (Eds.), *Interrelationships of Fishes* (pp. 85–115). Burlington: Academic Press.

Grande, L., & Bemis, W. E. (1998). A comprehensive phylogenetic study of amiid fishes (Amiidae) based on comparative skeletal anatomy. An

empirical search for interconnected patterns of natural history. *Society of Vertebrate Paleontology Memoir*, *4*, *i–X* 1–690.

Gross, J. B., & Hanken, J. (2008). Review of fate-mapping studies of osteogenic cranial neural crest in vertebrates. *Developmental Biology*, *317*, 389–400.

Hammarberg, F. (1937). Zur Kenntnis der ontogenetischen Entwicklung des Schädels von *Lepidosteus platystomus*. *Acta Zoologica*, *18*, 209–337.

Hilton, E. J. (2002a). *Osteology of the extant North American fishes of the genus Hiodon Lesueur, 1818 (Teleostei: Osteoglossomorpha: Hiodontiformes)*. Chicago: Field Museum of Natural History.

Hilton, E. J. (2002b). Observations on rostral canal bones of two species of *Acipenser* (Actinopterygii, Acipenseriformes). *Copeia*, *2002*, 213–219.

Hilton, E. J. (2005). Observations on the skulls of sturgeons (Acipenseridae): shared similarities of *Pseudoscaphirhynchus kaufmanni* and juvenile specimens of *Acipenser stellatus*. *Environmental Biology of Fishes*, *72*, 135–144.

Hilton, E. J., & Bemis, W. E. (1999). Skeletal variation in shortnose sturgeon (*Acipenser brevirostrum*) from the Connecticut River: Implications for comparative osteological studies of fossil and living fishes. In G. Arratia & H.-P. Schultze (Eds.), *Mesozoic Fishes 2 - Systematics and Fossil Record* (pp. 69–94). München, Germany: Verlag Dr. Friedrich Pfeil.

Hilton, E. J., & Bemis, W. E. (2012). External morphology of shortnose sturgeon *Acipenser brevirostrum* (Acipenseriformes: Acipenseridae) from the Connecticut river with notes on variation as a natural phenomenon. In B. Kynard, P. Bronzi, & H. Rosenthal (Eds.), *Life History and Behaviour of Connecticut River Shortnose and Other Sturgeons* (pp. 243–275). World Sturgeon Conservation Society.

Hilton, E. J., Dillman, C. B., Zhang, T., Zhang, L., & Zhuang, P. (2016). The skull of the Chinese sturgeon, *Acipenser sinensis* (Acipenseridae). *Acta Zoologica*, *97*, 419–432.

Hilton, E. J., & Forey, P. L. (2009). Redescription of †*Chondrosteus acipenseroides* Egerton, 1858 (Acipenseriformes, †Chondrosteidae) from the lower Lias of Lyme Regis (Dorset, England), with comments on the early evolution of sturgeons and paddlefishes. *Journal of Systematic Palaeontology*, *7*, 427–453.

Hilton, E. J., Grande, L., & Bemis, W. E. (2011). Skeletal anatomy of the Shortnose sturgeon, *Acipenser brevirostrum* Lesueur, 1818, and the systematics of sturgeons (Acipenseriformes, Acipenseridae). *Fieldiana Life and Earth Sciences*, *3*, 1–168.

Hirasawa, T., & Kuratani, S. (2015). Evolution of the vertebrate skeleton: Morphology, embryology, and development. *Zoological Letters*, *1*, 1–17.

Holčik, J. (1989). *The freshwater fishes of Europe, volume 1/II general introduction to fishes: Acipenseriformes* (469 p). Wiesbaden: AULA-Verlag.

Holmgren, N., & Stensiö, E. (1936). Kranium und Visceralskelett der Akranier, Cyclostomen und Fische. In L. Bolk, E. Göppert, E. Kallius, & W. Lubosch (Eds.), *Handbuch der vergleichenden Anatomie der Wirbeltiere* (pp. 233–499). Berlin und Wien: Urban & Schwarzenberg.

Huxley, T. H. (1857). The Croonian lecture: on the theory of the vertebrate skull. *Proceedings of the Royal Society of London*, *9*, 381–457.

Jiang, X., Iseki, S., Maxson, R. E., Sucov, H. M., & Morriss-Kay, G. M. (2002). Tissue origins and interactions in the mammalian skull vault. *Developmental Biology*, *241*, 106–116.

Jollie, M. (1980). Development of head and pectoral girdle skeleton and scales in *Acipenser*. *Copeia*, *1980*, 226–249.

Jollie, M. (1984). Development of the head and pectoral skeleton of *Polypterus* with a note on scales (Pisces: Actinopterygii). *Journal of Zoology*, *204*, 469–507.

Konstantinidis, P., Warth, P., Naumann, B., Metscher, B., Hilton, E. J., & Olsson, L. (2015). The developmental pattern of the musculature associated with the mandibular and hyoid arches in the Longnose gar, *Lepisosteus osseus* (Actinopterygii, Ginglymodi, Lepisosteiformes). *Copeia*, *103*, 920–932.

Krieger, J., Hett, A. K., Fuerst, P. A., Artyukhin, E., & Ludwig, A. (2008). The molecular phylogeny of the order Acipenseriformes revisited. *Journal of Applied Ichthyology*, *24*, 36–45.

Kuratani, S., Adachi, N., Wada, N., Oisi, Y., & Sugahara, F. (2013). Developmental and evolutionary significance of the mandibular arch and prechordal/premandibular cranium in vertebrates: revising the heterotopy scenario of gnathostome jaw evolution. *Journal of Anatomy*, *222*, 41–55.

Langille, R. M., & Hall, B. K. (1987). Development of the head skeleton of the Japanese medaka, *Oryzias latipes* (Teleostei). *Journal of Morphology*, *193*, 135–158.

Lauder, G. V. (1980). Evolution of the feeding mechanism in primitive actionopterygian fishes: a functional anatomical analysis of *Polypterus*, *Lepisosteus*, and *Amia*. *Journal of Morphology*, *163*, 283–317.

Leprévost, A., AzaÏs, T., Trichet, M., & Sire, J.-Y. (2016). Vertebral Development and Ossification in the Siberian Sturgeon (Acipenser Baerii), with New Insights on Bone Histology and Ultrastructure of Vertebral Elements and Scutes. *The Anatomical Record*.

Ludwig, A., Lippold, S., Debus, L., & Reinartz, R. (2009). First evidence of hybridization between endangered sterlets (*Acipenser ruthenus*) and exotic Siberian sturgeons (*Acipenser baerii*) in the Danube River. *Biological Invasions*, *11*, 753–760.

Maddin, H. C., Piekarski, N., Sefton, E. M., & Hanken, J. (2016). Homology of the cranial vault in birds: new insights based on embryonic fate-mapping and character analysis. *Royal Society Open Science*, *3*.

Mayden, R. L., & Kuhajda, B. R. (1996). Systematics, taxonomy, and conservation status of the endangered Alabama sturgeon, *Scaphirhynchus suttkusi* Williams and Clemmer (Actinopterygii, Acipenseridae). *Copeia*, *1996*, 241–273.

McAllister, D. E. (1968). The evolution of branchiostegals and associated opercular, gular, and hyoid bones, and the classification of teleostome fishes, living and fossil. *National Museum of Canada Bulletin Biological Series*, *77*, 1–239.

Moy-Thomas, J. A. (1933). Memoirs: notes on the development of the chondrocranium of *Polypterus senegalus*. *Quarterly Journal of Microscopical Science*, *76*, 209–229.

Nathanailides, C., Tsoumani, M., Papazogloy, A., & Paschos, I. (2002). Hatching time and post-hatch growth in Russian sturgeon *Acipenser gueldenstaedtii*. *Journal of Applied Ichthyology*, *18*, 651–654.

Nelson, G. J. (1969). Gill arches and the phylogeny of fishes: with notes on the classification of vertebrates. *Bulletin of the American Museum of Natural History*, *V 141*, 475–552.

Northcutt, R. G., & Gans, C. (1983). The genesis of neural crest and epidermal placodes: A reinterpretation of vertebrate origins. *The Quarterly Review of Biology*, *58*, 1–28.

Oken, L. (1807). Über die Bedeutung der Schädelknochen. Ein Programm beym Antritt der Professur an der Gesammt-Universität zu Jena. *Neue Leipziger Literaturzeitung*, *4*, 1–18.

Olsson, L., Falck, P., Lopez, K., Cobb, J., & Hanken, J. (2001). Cranial neural crest cells contribute to connective tissue in cranial muscles in the anuran amphibian, *Bombina orientalis*. *Developmental Biology*, *237*, 354–367.

Park, C., Lee Sang, Y., Kim, D. S., & Kwon, N. Y. (2013). Embryonic development of Siberian sturgeon *Acipenser baerii* under hatchery conditions: An image guide with embryological descriptions. *Fisheries and Aquatic Sciences*, *16*, 15–23.

Parker, W. K. (1881). On the structure and development of the skull in sturgeons (*Acipenser ruthenus* and *A. sturio*). *Proceedings of the Royal Society of London*, *32*, 142–145.

Patterson, C. (1982). Morphology and interrelationships of primitive actinopterygian fishes. *American Zoologist*, *22*, 241–259.

Pehrson, T. (1922). Some points in the cranial development of teleostomian fishes. *Acta Zoologica*, *3*, 1–63.

Pehrson, T. (1944). Some observations on the development and morphology of the dermal bones in the skull of *Acipenser* and *Polyodon*. *Acta Zoologica*, *25*, 27–48.

Pehrson, T. (1947). Some new interpretations of the skull in *Polypterus*. *Acta Zoologica*, *28*, 399–455.

Piekarski, N., Gross, J. B., & Hanken, J. (2014). Evolutionary innovation and conservation in the embryonic derivation of the vertebrate skull. *Nature Communications*, *5*, 5661.

Psenicka, M., Hadi Alavi, S. M., Rodina, M., Cicova, Z., Gela, D., Cosson, J., . . . Linhart, O. (2008). Morphology, chemical contents and physiology of chondrostean fish sperm: a comparative study between Siberian sturgeon (*Acipenser baerii*) and sterlet (*Acipenser ruthenus*). *Journal of Applied Ichthyology*, *24*, 371–377.

Rodríguez, A., & Gisbert, E. (2001). Morphogenesis of the eye of Siberian sturgeon. *Journal of Fish Biology*, *59*, 1427–1429.

Romeis, B. (1989). *Mikroskopische Technik* (697 p). München Wien Baltimore: Urban und Schwarzenberg.

Ruban, G. I. (1997). Species structure, contemporary distribution and status of the Siberian surgeon *Acipenser baerii*. *Environmental Biology of Fishes*, *48*, 221–230.

Ruban, G. I., & Zhu, B. (2010). *Acipenser baerii*. The IUCN Red List of Threatened Species.

Sabaj, M. H. (2016). Standard symbolic codes for institutional resource collections in herpetology and ichthyology: an online reference. Version 6.5 (16 August 2016). Washington, DC: American Society of Ichthyologists and Herpetologists. Retrieved from http://www.asih.org/

Santagati, F., & Rijli, F. M. (2003). Cranial neural crest and the building of the vertebrate head. *Nature Reviews Neuroscience*, *4*, 806–818.

Schmalhausen, O. I. (1991). The Russian sturgeon *Acipenser gueldenstaedtii* part II. Later prelarval development. In T. A. Dettlaff & S. G. Vassetzky (Eds.), *Animal Species for Developmental Studies* (pp. 67–88). Springer US.

Sefton, E. M., Piekarski, N., & Hanken, J. (2015). Dual embryonic origin and patterning of the pharyngeal skeleton in the axolotl (*Ambystoma mexicanum*). *Evolution & Development*, *17*, 175–184.

Sewertzoff, A. N. (1928). The head skeleton and muscles of *Acipenser ruthenus*. *Acta Zoologica*, *9*, 193–319.

Song, W., & Song, J.-K. (2012). Development of the lateral line system in juvenile Siberian sturgeon (*Acipenser baerii*). *Zoological Research*, *33*, 261–270.

Stengel, F. F. (1962). Untersuchungen am Kopf, besonders am Bänderapparat, des Sterlets (*Acipenser ruthenus*). *Revue Suisse de Zoologie*, *69*, 513–557.

Stone, L. S. (1926). Further experiments on the extirpation and transplantation of mesectoderm in *Amblystoma punctatum*. *Journal of Experimental Zoology*, *44*, 95–131.

Taylor, W. R., & van Dyke, G. C. (1985). Revised procedures for staining and clearing small fishes and other vertebrates for bone and cartilage study. *Cybium*, *9*, 107–119.

Tranah, G., Campton, D. E., & May, B. (2004). Genetic evidence for hybridization of Pallid and Shovelnose sturgeon. *Journal of Heredity*, *95*, 474–480.

van Wijhe, J. W. (1882). Ueber das Visceralskelett und die Nerven des Kopfes der Ganoiden und von *Ceratodus*. *Niederländisches Archiv für Zoologie*, *5*, 207–320.

Vasil'eva, E. D., Vasil'ev, V. P., Shedko, S. V., & Novomodny, G. V. (2009). The revision of the validity of genus *Huso* (Acipenseridae) based on recent morphological and genetic data with particular reference to the Kaluga *H. dauricus*. *Journal of Ichthyology*, *49*, 861–867.

Véran, M. (1988). Les éléments accessories de l'arc hyoïdien des poisons téléostomes (Acanthodiens et Osteichthyens) fossils et actuels. *Mémoires du Muséum National D'Histoire Naturelle*, *54*, 1–98.

Wiley, E. O. (1976). *The phylogeny and biogeography of fossil and recent gars (Actinopterygii: Lepisosteidae)* (111 p). Lawrence, Kansas: The University of Kansas Museum of Natural History.

Williot, P., Sabeau, L., Gessner, J., Arlati, G., Bronzi, P., Gulyas, T., & Berni, P. (2001). Sturgeon farming in Western Europe: recent developments and perspectives. *Aquatic Living Resources*, *14*, 367–374.

Zelazowska, M. (2010). Formation and structure of egg envelopes in Russian sturgeon *Acipenser gueldenstaedtii* (Acipenseriformes: Acipenseridae). *Journal of Fish Biology*, *76*, 694–706.

Zhou, Z. (1992). Review on *Peipiaosteus* based on new materials of *P. pani*. *Vertebrata Palasiatica*, *30*, 85–101.

How to cite this article: Warth P, Hilton EJ, Naumann B, Olsson L, Konstantinidis P. Development of the skull and pectoral girdle in Siberian sturgeon, *Acipenser baerii*, and Russian sturgeon, *Acipenser gueldenstaedtii* (Acipenseriformes: Acipenseridae). *Journal of Morphology*. 2017;00:1–25. https://doi.org/10.1002/jmor.20653